Enlcosure 3 Contains Proprietary Information to be Withheld from Public Disclosure Pursuant to 10 CFR 2.390

PSEG Nuclear LLC
P.O. Box 236, Hancocks Bridge, NJ 08038-0236

PSEG
Nuclear LLC

10 CFR 50.90

DEC 19 2017

LR-N17-0186
LAR H17-03

U.S. Nuclear Regulatory Commission
ATTN: Document Control Desk
Washington, DC 20555-0001

Hope Creek Generating Station
Renewed Facility Operating License No. NPF-57
NRC Docket No. 50-354

Subject: **RESPONSE TO REQUEST FOR ADDITIONAL INFORMATION REGARDING LICENSE AMENDMENT REQUEST FOR MEASUREMENT UNCERTAINTY RECAPTURE POWER UPRATE (CAC NO. MF9930)**

References
1. PSEG letter to NRC, "License Amendment Request for Measurement Uncertainty Recapture (MUR) Power Uprate," dated July 7, 2017 (ADAMS Accession No. ML17188A260)
2. NRC e-mail to PSEG, "Final Request for Additional Information - Steam Dryer Analysis for Hope Creek MUR," dated December 14, 2017 (ADAMS Accession No ML17348A997)

In the Reference 1 letter, PSEG Nuclear LLC (PSEG) submitted a license amendment request for Hope Creek Generating Station (HCGS). The proposed amendment will increase the rated thermal power (RTP) level from 3840 megawatts thermal (MWt) to 3902 MWt, and make Technical Specification (TS) changes as necessary to support operation at the uprated power level.

In Reference 2, the U.S. Nuclear Regulatory Commission staff requested PSEG to submit the document CDI Technical Note (TN) 16-23P to support the NRC review of Reference 1.

This letter provides a non-proprietary version of the requested document in Enclosure 1 and a proprietary version in Enclosure 3.

Enclosure 3 contains proprietary information as defined by 10 CFR 2.390. Continuum Dynamics, Inc. (CDI), as the owner of the proprietary information, has executed an affidavit (provided in Enclosure 2) identifying that the proprietary information has been handled and classified as proprietary, is customarily held in confidence, and has been withheld from public disclosure. CDI requests that the proprietary information in Enclosure 3 be withheld from public disclosure, in accordance with the requirements of 10 CFR 2.390(a)(4).

PSEG has determined that the information provided in this submittal does not alter the conclusions reached in the 10 CFR 50.92 no significant hazards determination previously submitted. In addition, the information provided in this submittal does not affect the bases for concluding that neither an environmental impact statement nor an environmental assessment needs to be prepared in connection with the proposed amendment.

No new regulatory commitments are established by this submittal. If you have any questions or require additional information, please do not hesitate to contact Mr. Brian Thomas at (856) 339-2022.

I declare under penalty of perjury that the foregoing is true and correct.

Executed on 12/19/17
(Date)

Respectfully,

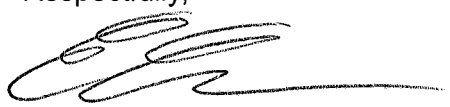

Eric Carr
Site Vice President
Hope Creek Generating Station

Attachment

1. Response to EMIB Request for Additional Information Regarding MUR Power Uprate

Enclosures

1. CDI Technical Note (TN) 16-23NP, Stress Evaluation of Hope Creek Unit 1 Steam Dryer at MUR Conditions Using Perforated Plate Damping - Non-Proprietary

2. CDI Affidavit supporting the withholding of information in Enclosure 3 from public disclosure

3. CDI Technical Note (TN) 16-23P, Stress Evaluation of Hope Creek Unit 1 Steam Dryer at MUR Conditions Using Perforated Plate Damping - Proprietary

cc: Mr. D. Dorman, Administrator, Region I, NRC
Ms. L. Regner, Project Manager, NRC
NRC Senior Resident Inspector, Hope Creek
Mr. P. Mulligan, Chief, NJBNE
Mr. L. Marabella, Corporate Commitment Tracking Coordinator
Mr. T. MacEwen, Hope Creek Commitment Tracking Coordinator

Response to EMIB Request for Additional Information Regarding MUR Power Uprate

RESPONSE TO REQUEST FOR ADDITIONAL INFORMATION
LICENSE AMENDMENT REQUEST FOR MEASUREMENT UNCERTAINTY RECAPTURE (MUR) POWER UPRATE
PSEG NUCLEAR LLC (PSEG)
HOPE CREEK GENERATING STATION (HOPE CREEK)
DOCKET NO. 50-354

By letter dated July 07, 2017 (Agencywide Documents Access and Management System Accession No. ML17188A260), PSEG Nuclear LLC (the licensee) submitted a License Amendment request for Hope Creek Generating Station (Hope Creek). The amendment would revise the Renewed Facility Operating Licenses (RFOLs) and Technical Specifications (TSs) to implement a measurement uncertainty recapture (MUR) power uprate. Specifically, the amendments would authorize an increase in the maximum licensed thermal power level from 3,840 megawatts thermal (MWt) to 3,902 MWt, which is an increase of approximately 1.61 percent above the current thermal power, or an increase of 19 percent above the original licensed thermal power (3293 MWt.).

To complete its review, the Nuclear Regulatory Commission (NRC) staff requests the following additional information.

EMIB-01

In enclosure 1 to LAR H17-03, Section 3.4.2 on Adverse Flow Effects, the licensee references steam dryer stress analysis document, but this document was not provided to the NRC. The steam dryer analysis reveals the low margin due to an Acoustic Circuit Model (ACM) code error discovered in 2015. The licensee is requested to provide the document, CDI Technical Note (TN) 16-23P, "Steam Dryer Analysis" on the docket for NRC review and to allow the NRC staff to reach a safety conclusion regarding the continued structural integrity of the steam dryer and verify the margin for high cycle fatigue stresses due to adverse flow effects.

RESPONSE:

Non-proprietary and proprietary versions of CDI Technical Note (TN) 16-23P are provided in Enclosures 1 and 3 of this letter respectively.

CDI Technical Note (TN) 16-23NP, Stress Evaluation of Hope Creek Unit 1 Steam Dryer at MUR Conditions Using Perforated Plate Damping
Non-Proprietary

This is the non-proprietary version of Enclosure 3 of this letter which has the proprietary information removed. Portions of the document that have been removed are indicated by white space inside open and closed brackets as shown here [[(3)]].

This document does not contain Continuum Dynamics, Inc. Proprietary Information

C.D.I. Technical Note 16-23NP

Stress Evaluation of Hope Creek Unit 1 Steam Dryer at MUR Conditions Using Perforated Plate Damping

Revision 0

Prepared by

Continuum Dynamics, Inc.
34 Lexington Avenue
Ewing, NJ 08618

Prepared under Purchase Order No. 4500955256 for

Nuclear Business Unit, PSEG Nuclear LLC
Materials Center, Alloway Creek Neck Road
Hancocks Bridge, NJ 08038

Prepared by

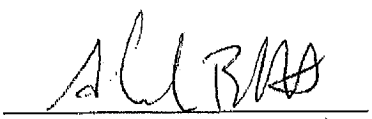

Alexander H. Boschitsch

Reviewed by

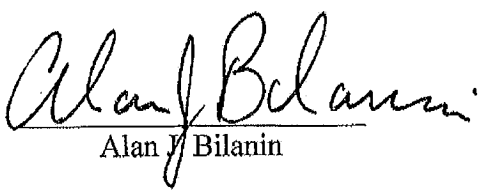

Alan J. Bilanin

January 2017

Executive Summary

The stresses on the Hope Creek steam dryer are calculated at MUR conditions with the effect of perforated plate damping (PPD) taken into account. [[

(3)]]

The current stress evaluation does not include the effect known as [[(3)]]; a stress evaluation with this effect is given in [2]. Except for the inclusion of PPD and the evaluation at MUR rather than CLTP conditions, the stress assessment is identical to that reported in [3]. These stress predictions account for all the end-to-end biases and uncertainties in the loads model [4] and finite element analysis [5]. To account for frequency uncertainties in the finite element model, the stresses are also computed for loads that are shifted in the frequency domain between ±10% in 2.5% increments. From this assessment the limiting stress ratios obtained at CLTP and MUR, with and without PPD in the HC1 steam dryer are as follows:

Load	PPD	Minimum Stress Ratio No Freq. Shifting		Minimum Stress Ratio with Freq. Shifting	
		SR-P	SR-a	SR-P	SR-a
CLTP	None	1.33	1.12	1.27	1.07
MUR	None	1.33	1.08	1.26	1.04
CLTP	42.5%	1.33	1.14	1.27	1.08
MUR	42.5%	1.33	1.10	1.26	1.05

The minimum alternating stress ratio increases from SR-a=1.04 to SR-a=1.05 when PPD is applied. At other locations with SR-a<2, stress reductions of up to 2.6% are observed; when considering the locations with SR-a<5, stress reductions of up to 23% are noted. These reductions are consistent with those at other plants, but do not occur at the limiting location for the HC1 dryer. The limiting location is the same both with and without PPD and lies on the weld connecting the backing bar to the middle hood. All stress ratios meet the ASME code allowable.

Table of Contents

Nomenclature

ACM	acoustic circuit model
ASME	American Society of Mechanical Engineers
B&PV	Boiler and Pressure Vessel
CDI	Continuum Dynamics, Inc.
CLTP	current licensed thermal power
EPU	extended power uprate
f_{sw}	weld factor
HC1	Hope Creek Unit 1
MASR	minimum alternating stress ratio
MSL	main steam line
MUR	measurement uncertainty recovery
NRC	Nuclear Regulatory Commission
Pb	bending stress intensity
Pm	membrane stress intensity
PPD	perforated plate damping
PSD	power spectral density
RMS	root mean square
RPS	reduced point set
Sa	service limit for alternating stress intensity
S_{alt}	alternating stress intensity
Sm	service limit for membrane stress intensity
SR-a	alternating stress ratio
SR-P	peak stress ratio
USR	upper support ring
[[	(3)]]
WF	weld factor
1D	one-dimensional

1. Introduction & Approach Overview

The steam dryer loads due to acoustic pressure fluctuations in the main steam lines (MSLs) are potentially damaging and the cyclic stresses from these loads can produce fatigue cracking if loads are sufficiently high. The industry has addressed this problem with physical modifications to the dryers, as well as a program to define steam dryer loads and their resulting stresses. The present report evaluates the stresses for the Hope Creek Unit 1 (HC1) nuclear plant steam dryer at the planned Measurement Uncertainty Recovery (MUR) condition, which corresponds to a power increase relative to CLTP of, at most, 1.72%.

The present stress analysis complements and differs from prior stress assessments of the HC1 dryer by accounting for the effect of perforated plate damping (PPD), which has been included in the stress analysis for other plants (e.g., [6] & [7]), but not for the HC1 dryer. In [3], an identical stress analysis was carried out for CLTP conditions that omitted PPD and yielded a minimum alternating stress ratio (MASR) of 1.07. Scaling this result to MUR conditions estimates a MASR of 1.04, which while above the ASME limit of 1.0, warrants consideration of alternate methods that account for known dissipation mechanisms. The hope is to increase margin and/or restrict high stress locations to sites or welds that can be readily inspected. In [2] [[

$^{(3)}$]].

PPD arises when a perforated plate experiences vibration along its normal direction while simultaneously subject to steady state flow through the perforation holes. In steam dryers this situation arises for the plates immediately ahead (inlet) and aft (exit) of the vane bank assemblies. The force is proportional to the product of the mean velocity through the perforation holes and normal plate velocity. It therefore acts as a resistive force and increases with the approach velocity and inverse of open area ratio. Since the use of PPD was permitted under previous steam dryer assessments for power uprates [6, 7] its use is reasonable for the comparatively smaller HC1 MUR uprate. Note that the contributions of perforated plate damping were also quantified by experiment [8] and only 42.5% of the theoretical PPD is used which is also well below the levels observed in experiment. PPD mainly affects the response of the perforated plates and parts to which they are attached such as the hood supports and vane bank support. For the HC1 unit at CLTP, the limiting MASR locations involve the hood and hood supports; hence PPD is expected to alleviate stresses on those parts. Other high stress locations occurring on the drain channel/skirt welds are located further away from the perforated plates and any changes in stress at these locations are expected to be small. These welds are readily accessible for inspection and have not experienced damage to date, despite 8+ years of operation at CLTP.

The load combination considered here corresponds to normal operation (the Level A Service Condition) and includes fluctuating pressure loads developed from HC1 main steam line data, and weight. Level B service conditions, which include seismic loads, are not included in this evaluation. The fluctuating pressure loads, induced by the flowing steam, are predicted at the

CLTP condition using a separate acoustic circuit analysis of the steam dome and main steam lines [9]. MUR stresses are estimated by simple scaling of the flow-induced CLTP stresses by velocity squared or, in this case, $1.0172^2=1.035$. A potential for resonances exists at both CLTP and MUR conditions and so the bias and uncertainty for a resonant peak have been applied to the loads over the 116-120 Hz frequency interval over which a putative resonance would emerge.

The stress analysis is carried out in the frequency domain, which confers a number of useful computational advantages over a time-accurate transient analysis including the ability to assess the effects of frequency scaling in the loads without the need for additional finite element calculations. For additional details of this approach as well as of the HC1 finite element model, the manner in which the acoustic loads are applied to the dryer, the post-processing of the results to obtain stress intensities and stress ratios suitably adjusted at welds to establish compliance with the ASME B&PV Code (Section III, subsection NG) [10], the reader is referred to [3]. Except for the application of PPD and scaling to MUR conditions the stress evaluation is performed in the same manner as in [3]. Additional details of PPD applied to the HC1 steam dryer are provided below.

Section 2 summarizes the stress results using PPD by tabulating the highest maximum and alternating stress intensities and presenting contour plots of these stresses to indicate which points on the dryer experience significant stress concentration and/or modal response (Section 2.1). Comparisons of the stresses against allowable values, accounting for stress type (maximum and alternating) and location (on or away from a weld) are also provided in terms of stress ratios in Section 2.2. Section 2.3 examines the spectral content of select nodes and the dominant frequency distribution over the dryer. Section 3 compares the stresses with and without PPD. It is shown that while at some locations near the perforated plates the stress are reduced by more than 20%, the limiting stress locations only change by about 1%. The limiting maximum and alternating stress ratios at MUR are estimated as SR-P=1.26 and SR-a=1.05. The overall stress distributions and their frequency content with and without PPD are found to be similar.

1.1 Perforated Plate Damping Model

[[

(1)

(2)

(3)

[(3)]]

[[

$^{(3)}$]]

[[

[3]]]

Figure 1. [[

[3]]]

Table 1. Damping properties of perforated plates.

[[

[3]]]

2. Stresses at MUR Using PPD

The present section reports the stresses obtained when PPD is used. Results are presented both at nominal conditions (no frequency shift) and with frequency shift included. As done in [3], frequency shifts are performed at 2.5% increments. The effects of frequency shifts can be conservatively accounted for by identifying the maximum stress (Section 2.1) or minimum stress ratio (Section 2.2) at every node, where the minimum is taken over all the frequency shifts considered (including the nominal or 0% shift case). The stress tables also report the dominant frequencies in the stress response estimated by identifying the Fourier coefficient with the biggest amplitude. When frequency shifting is performed the pre-shift frequency is reported; so, for example, a reported 50 Hz frequency with +10% frequency shift corresponds to a stress response peak at 55 Hz.

The tabulated stresses and stress ratios are obtained using a 'blanking' procedure that is designed to prevent reporting a large number of high stress nodes from essentially the same location on the structure. Details of the blanking process are given in Section 5 of [3]. Here it suffices to note that a node appearing in the stress table actually represents the limiting stress or stress ratio within a 10 inch neighborhood and its 3 mirror images across the x- and y- symmetry planes.

2.1 General Stress Distribution and High Stress Locations

The maximum stress intensities obtained by post-processing the ANSYS stress histories for MUR at nominal frequency and with frequency shift operating conditions are listed in Table 2. Contour plots of the stress intensities over the steam dryer structure are shown in Figure 2 (maximum stress over all nine frequency shifts including nominal). The figures are oriented to emphasize the high stress regions. Note that these stress intensities *do not* account for weld factors but do include end-to-end bias and uncertainty. Further, it should be noted that since the allowable stresses vary with location, stress intensities do not necessarily correspond to regions of primary structural concern. Instead, structural evaluation is more accurately made in terms of the stress ratios which compare the computed stresses to allowable levels with due account made for stress type and weld factors. Comparisons on the basis of stress ratios are made in Section 2.2.

The general stress state in terms of stress intensities and low stress ratio locations is very similar to the ones reported previously for CLTP without PPD [3]. For the peak stresses, Pm and Pm+Pb, many of the nodes are dominated by the static component which does not change with the acoustic loads. The maximum stress intensities in most areas are low (less than 500 psi, or 5% of the most conservative critical stress). For the membrane stresses (Pm) the high stress regions tend to occur at: (i) the inner hoods; (ii) the outermost portion of the inner hood near the connection to the closure plate; (iii) the weld joining the skirt and the upper support ring near the supports; and (iv) the central base plate/vane bank junction. For most locations the stress is dominated by static stresses as evidenced by the small alternating stresses in the rightmost columns in the table. The closure plates and regions in the vicinity of where they connect to adjacent hoods or vane banks, experience high stresses since they restrain any deflection of the adjacent vane banks.

The membrane + bending stress (P m+Pb) distributions show a pronounced m odal response pattern, notably over the drain channels. Howeve r, except for the drain channel/skirt welds the highest stress locations are still dom inated by the static com ponent as confirmed by comparing the Pm+Pb and Salt colum ns in Table 2. Stre ss concentrations are visible near the hood supports, at the bottoms of the hoods, near the tops of the closure plates and along the skirt/drain channel welds.

The highest alternating stress without freque ncy shifting is 6243 psi occurring on the weld joining the middle hood and backing bar. This increases to 6566 psi when frequency shifting is included with the lim iting shift bein g +2.5%. Th e highest alternating st ress intensity at a non-weld location is 6444 psi on the inner hood (with frequency shiftin g). The alternating stress intensity contour plots in Figure 2d-e essentially record the modes excited by this signal, which here are seen to primarily involve the inner and middle hoods which, though not directly exposed to the main MSL pressure fluctu ations (like the outer hoods are) are of th inner construction and therefore exhibit a significant response.

Table 2a. Locations with highest predicted stress intensities at MUR and PPD - no frequency shift.

Stress Category	Location		Location (in)				Stress Intensities (psi)			Dom. Freq. (Hz)
		Weld	x	y	z	node	Pm	Pm+Pb	S_{alt}	
Pm	Hood	No	109	-27.6	95.3	44886	6764	9587	1310	46.7
"	Backing Bar/Hood Support/Mid Cover Plate	Yes	0	-38.4	7.5	79684	5068	5126	2779	48.7
"	Inner Side Panel/Vane Bank/Mid Cover Plate	Yes	-118.8	14.4	7.5	85994	4593	6335	868	46.9
"	Hood Support/Mid Cover Plate/Backing Bar	Yes	59.5	38.4	7.5	86958	4523	4722	2512	47.7
"	Skirt/Skirt Ext	Yes	118.7	-5.9	-2	91960	4459	6526	1053	47.7
Pm+Pb	Skirt/Cap Strip/Skirt Ext	Yes	118.8	0.6	-2	88325	2579	10505	1671	46.8
"	Hood	No	109	-27.6	95.3	44886	6764	9587	1310	46.7
"	Backing Bar/Hood	Yes	-29.1	69.9	8.5	87919	732	6673	6243	49.0
"	Drain Channel/Bottom Skirt	Yes	118.2	12	-94.2	90843	1761	6666	4001	31.7
"	Drain Channel/Bottom Skirt	Yes	-73.8	93.1	-94.2	90834	2216	6502	4226	47.3
S_{alt}	Backing Bar/Hood	Yes	-29.1	69.9	8.5	87919	732	6673	6243	49.0
"	Hood	No	-30.2	68.9	35.2	37937	1242	5583	5297	49.0
"	Backing Bar/Hood	Yes	-29.5	38.4	8.5	85224	681	5532	5200	47.7
"	Hood	No	28.4	67.3	52.2	37238	1430	5502	5194	49.0
"	Hood	No	-24.2	64.9	69	37916	1330	5486	5157	49.0

Table 2b. Locations with highest predicted stress intensities taken over all frequency shifts at MUR and PPD.

Stress Category	Location	Weld	Location (in)				Stress Intensities (psi)			% Freq. Shift	Dom. Freq. (Hz)
			x	y	z	node	Pm	Pm+Pb	S_{alt}		
Pm	Hood	No	109	-27.6	95.3	44886	6842	9587	1377	10	48.7
"	Hood Support/Mid Cover Plate/Backing Bar	Yes	0	38.4	7.5	86960	5368	5418	3169	-10	48.6
"	Hood Support/Vane Bank/Mid Cover Plate	Yes	0	22.9	7.5	93159	5264	5299	3949	10	36.8
"	KT1-444/Hood	Yes	109.8	-38.4	9.5	92106	5027	5028	2549	10	48.6
"	Skirt/Skirt Ext	Yes	118.7	-5.9	-2	91960	4919	7152	1498	5	48.7
Pm+Pb	Skirt/Cap Strip/Skirt Ext	Yes	118.8	0.6	-2	88325	2951	11048	1996	-2.5	22.4
"	Hood	No	109	-27.6	95.3	44886	6842	9587	1377	0	48.7
"	Bottom Skirt/Drain Channel	Yes	73.8	-93.1	-94.2	93833	2319	8247	5988	10	28.4
"	Drain Pipe/Skirt	Yes	88.2	79.6	-20.5	91083	2718	7665	2284	10	48.7
"	Bottom Skirt/Drain Channel	Yes	-118.2	-12	-94.2	93758	2266	7416	4925	5	47.3
S_{alt}	Backing Bar/Hood	Yes	-29.1	69.9	8.5	87919	923	6983	6566	2.5	47.7
"	Hood	No	83.4	35.9	50.9	40188	3727	6843	6444	10	48.7
"	Backing Bar/Hood	Yes	30	38.4	8.5	88060	1258	6630	6194	-2.5	48.6
"	Hood Support/Hood	Yes	0	-36.1	49.6	80664	2793	6558	6148	10	36.8
"	Bottom Skirt/Drain Channel	Yes	73.8	-93.1	-94.2	93833	2319	8247	5988	10	28.4

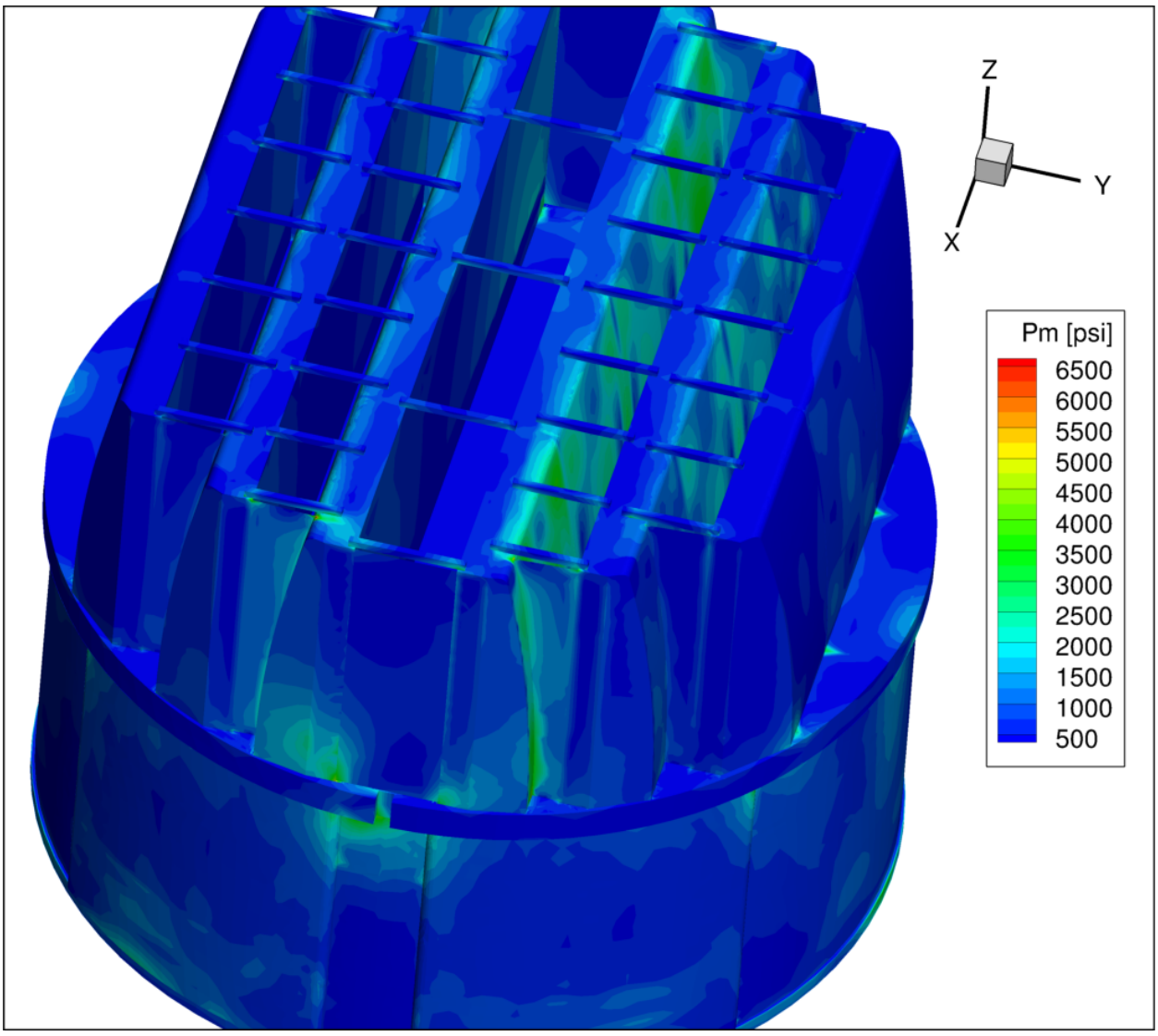

Figure 2a. Contour plot of m aximum membrane stress intensity, Pm, for MUR with frequency shifts. The recorded stress at a node is the maximum value taken over all frequency shifts. The maximum stress intensity is 6,842 psi.

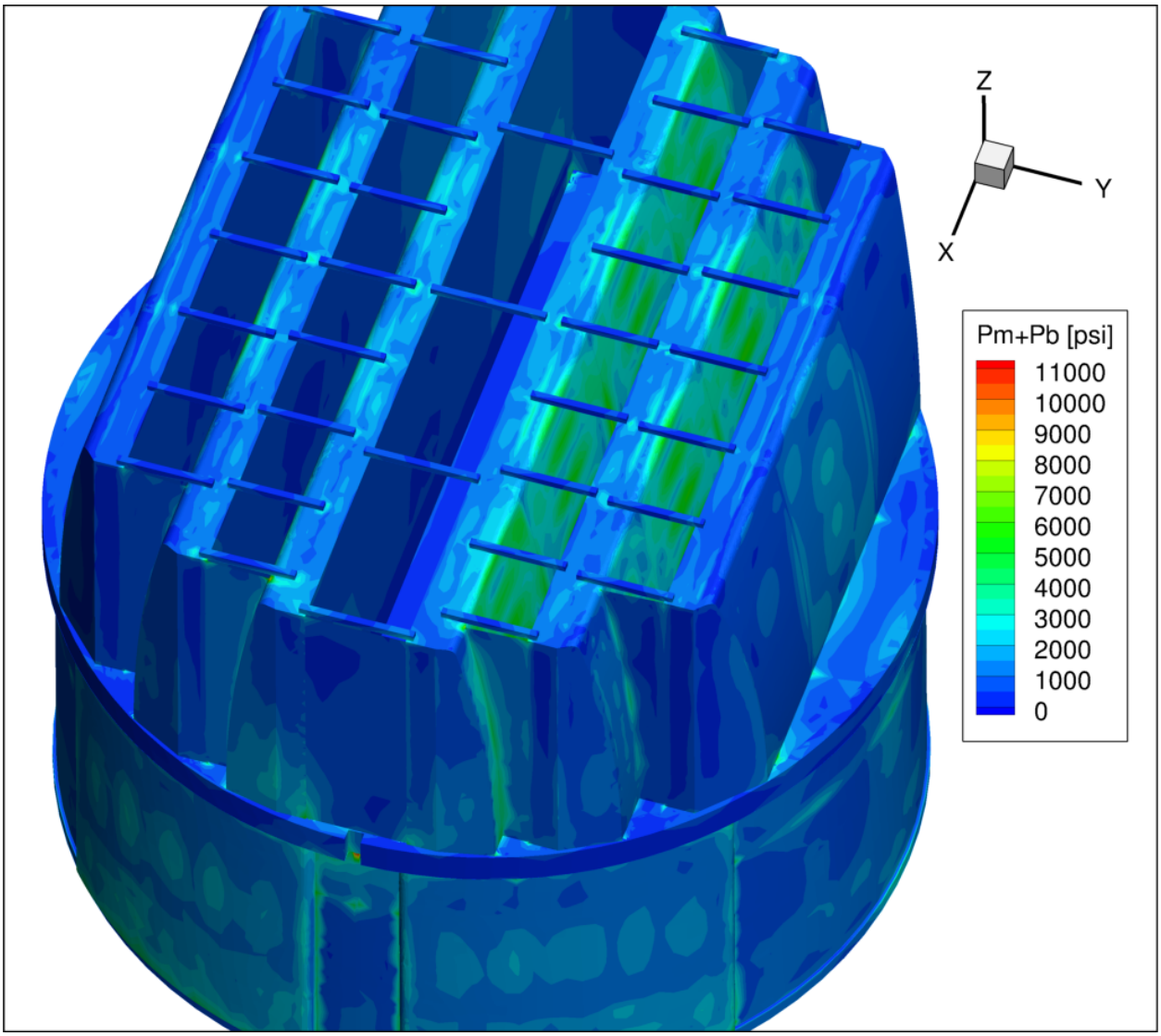

Figure 2b. Contour plot of maximum membrane+bending stress intensity, Pm+Pb, for MUR with frequency shifts. The recorded stress at a node is the maximum value taken over all frequency shifts. The maximum stress intensity is 11,048 psi. First view.

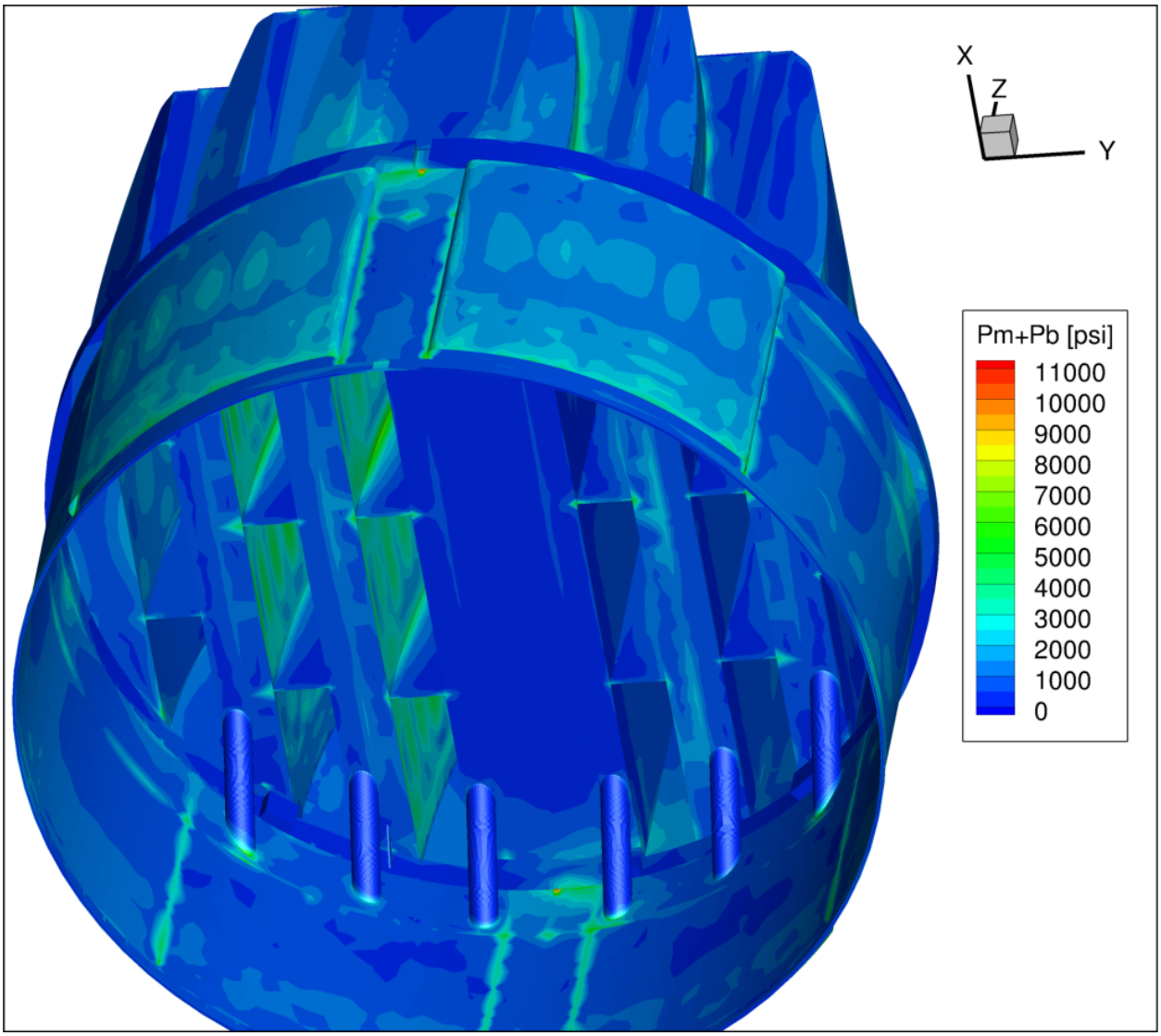

Figure 2c. Contour plot of maximum membrane+bending stress intensity, Pm+Pb, for MUR with frequency shifts. This second view from beneath reveals high stress and modal response of the hood/hood support junctions.

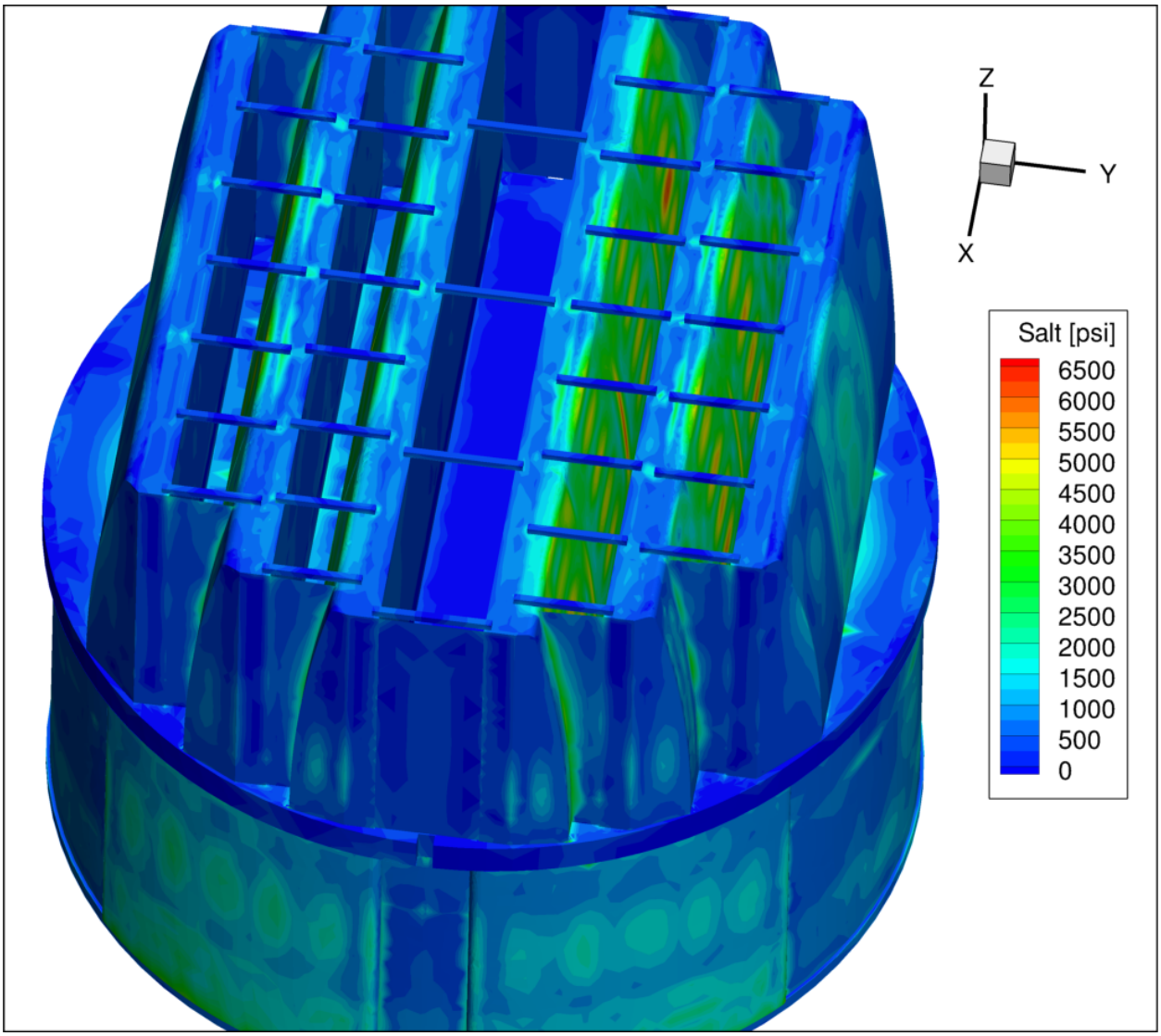

Figure 2d. Contour plot of alternating stress intensity, S_{alt}, for MUR with frequency shifts. The recorded stress at a node is the maximum value taken over all frequency shifts. The maximum alternating stress intensity is 6,566 psi. First view.

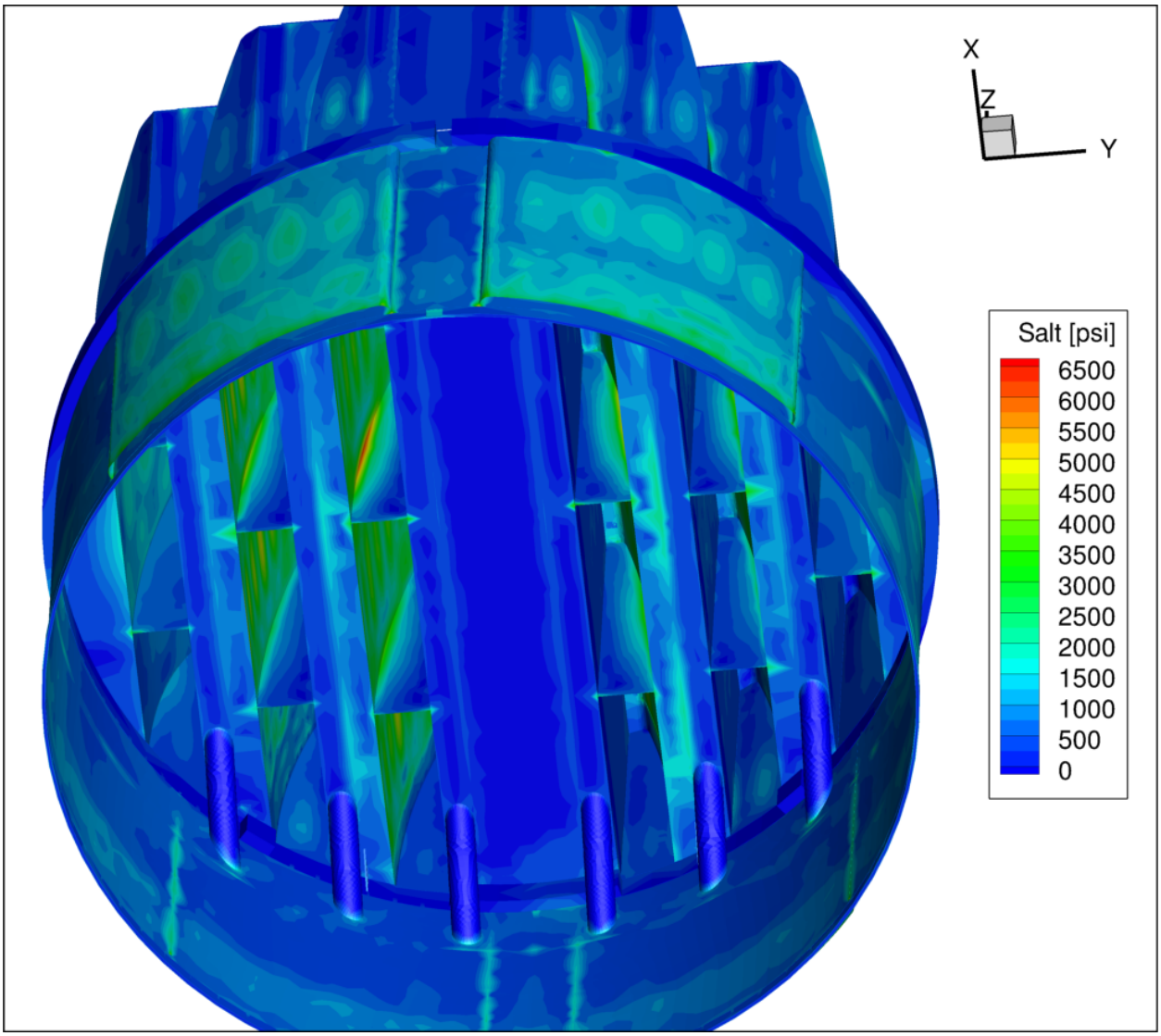

Figure 2e. Contour plot of alternating stress intensity, S_{alt}, for MUR with frequency shifts. This second view from beneath reve als more of the high stress regions on the hood/hood support junctions.

2.2 Load Combinations and Allowable Stress Intensities

The stress ratios computed for MUR at nominal frequency (no frequency shift) and with frequency shifting are listed in Table 3 and Table 4 respectively. The stress ratios are grouped according to type (SR-P for maximum membrane and membrane+bending stress, SR-a for alternating stress) and location (away from welds or on a weld). At nominal frequency shift the minimum peak stress ratio, SR-P=1.33, and occurs at the junction of the skirt and USR. At this condition, the dryer stress state is effectively governed by the weight-induced static stress field. This is clear from Table 3b where the corresponding alternating stress ratio is SR-a=4.11. The limiting peak stress ratio SR-P=1.26, occurs with the -2.5% shift and occurs at the same location as with no frequency shift. In [3], the limiting peak stress ratio also occurred at this location with SR-P=1.27 at CLTP, and had the same dominant 22.4 Hz frequency.

The minimum alternating stress ratio at any frequency shift, SR-a=1.05, occurs on the weld joining the bottom of the middle hood and backing bar. A similar stress state occurs on the inner hood/backing bar weld with SR-a=1.11. The third and fifth lowest alternating stress ratios occur on the inner hood/hood support junction. The fourth lowest alternating stress ratio is SR-a=1.15 and occurs at the bottom of the drain channel/skirt weld. These five locations comprise three distinct weld configurations: (a) hood/backing bar weld; (b) hood/hood support weld and (c) drain channel/skirt weld. All of the first 21 limiting alternating stress ratio locations with SR-a≤1.71 fall into one of these three categories. These are depicted in Figure 3f-h which identifies the 21 limiting nodes listed in Table 4c and also displays all nodes with SR-a<4 without blanking. The limiting alternating stress ratios with and without frequency shifts (SR-a=1.10 and 1.05 respectively) differ by less than 5%. Table 4d shows the remaining RPS locations with alternating stress ratios below 2.0 which introduces two new distinct weld configurations each having limiting SR-a=1.74. These are: (d) the weld connecting the inner hood and outer plenum plate (also referred to as the closure plate) (location 23); and (e) the junction between the inner vane bank/hood support/inner base plate (location 22). Virtually all locations are characterized by a dominant frequency occurring at either at 36.8 Hz or in the narrow range 47.7-48.7 Hz. These signals are prominent in the acoustic loads.

These observations closely follow those in [3] without PPD; further comparisons between the results with and without PPD are presented in Section 4.

Table 3a. Limiting non-weld locations at MUR with no frequency shift. Stress ratios are grouped according to stress type (maximum – SR-P; or alternating – SR-a)..

Stress Ratio	Location	Location (in.)			node	Stress Intensity (psi)			Stress Ratio		Dom. Freq. (Hz)
		x	y	z		Pm	Pm+Pb	S_{alt}	SR-P	SR-a	
SR-P	1. Outer portion of inner hood (top near closure plate)	109	-27.6	95.3	44886	6764	9587	1310	2.5	9.44	46.7
SR-a	1. Middle Hood	-30.2	68.9	35.2	37937	1242	5583	5297	4.54	2.33	49.0
"	2. Middle Hood	28.4	67.3	52.2	37238	1430	5502	5194	4.61	2.38	49.0
"	3. Middle Hood	-24.2	64.9	69	37916	1330	5486	5157	4.62	2.40	49.0
"	4. Middle Hood	-29.6	69.7	20.3	37971	910	5082	4804	4.99	2.57	49.0
"	5. Middle Hood	-27.6	62	84.6	37967	983	5001	4678	5.07	2.64	49.0
"	6. Middle Hood	34.2	64.9	68.8	37263	1135	4975	4675	5.10	2.64	49.0
"	7. Middle Hood	18.8	68.9	35.9	37299	1294	4767	4489	5.32	2.75	48.2
"	8. Inner Hood	30.4	33.5	68.2	42011	1127	4768	4472	5.32	2.76	47.7

Table 3b. Limiting peak stress ratios, SR-P, on welds at MUR with no frequency shift.

Location	Location (in.)				Stress Intensity (psi)			Stress Ratio		Dom. Freq. (Hz)
	x	y	z	node	Pm	Pm+Pb	S_{alt}	SR-P	SR-a	
1. Skirt/Cap Strip/Skirt Ext	118.8	0.6	-2	88325	2579	10505	1671	1.33	4.11	46.8
2. Closure Plate/Hood	108.4	27.9	94.9	85409	5961	8753	2263	1.56	3.03	47.7
3. Backing Bar/Hood Support/Mid Cover Plate	0	-38.4	7.5	79684	5068	5126	2779	1.83	2.47	48.7
4. Inner Side Panel/Vane Bank/Mid Cover Plate	-118.8	14.4	7.5	85994	4593	6335	868	2.02	7.92	46.9
5. Hood Support/Mid Cover Plate/Backing Bar	59.5	38.4	7.5	86958	4523	4722	2512	2.05	2.73	47.7
6. Backing Bar/Hood	-29.1	69.9	8.5	87919	732	6673	6243	2.09	1.10	49.0
7. Drain Channel/Bottom Skirt	118.2	12	-94.2	90843	1761	6666	4001	2.09	1.72	31.7

Table 3c. Limiting alternating stress ratios, SR-a, on welds at MUR with no frequency shift.

Location	Location (in.)				Stress Intensity (psi)			Stress Ratio		Dom. Freq. (Hz)
	x	y	z	node	Pm	Pm+Pb	S_{alt}	SR-P	SR-a	
1. Backing Bar/Middle Hood	-29.1	69.9	8.5	87919	732	6673	6243	2.09	1.10	49.0
2. Backing Bar/Inner Hood	-29.5	38.4	8.5	85224	681	5532	5200	2.52	1.32	47.7
3. Backing Bar/Middle Hood	-16.5	69.9	8.5	87922	1106	5222	4887	2.67	1.41	49.0
4. Drain Channel/Bottom of Skirt	-73.8	93.1	-94.2	90834	2216	6502	4226	2.14	1.63	47.3
5. Backing Bar/Inner Hood	-42.3	38.4	8.5	85227	1323	4560	4217	3.06	1.63	47.7
6. Hood Support/Inner Hood(a)	0	36.1	49.6	88022	1788	4275	4054	3.26	1.69	47.7
7. Hood Support/Middle Hood(a)	0	68.7	38.4	87904	1558	4243	4031	3.29	1.70	45.3
8. Drain Channel/Bottom of Skirt	118.2	12	-94.2	90843	1761	6666	4001	2.09	1.72	31.7
9. Backing Bar/Middle Hood	42.1	69.9	8.5	87826	1244	4210	3979	3.31	1.73	49.0
10. Hood Support/Middle Hood(a)	0	67.1	53.3	87900	1741	4272	3921	3.26	1.75	45.0
11. Backing Bar/Inner Hood	17.2	38.4	8.5	88057	1306	4176	3851	3.34	1.78	47.7
12. Backing Bar/Inner Hood	-81.5	38.4	8.5	85461	582	4051	3707	3.44	1.85	47.7
13. Hood Support/Inner Hood(a)	0	-37.2	38.4	80716	1589	4028	3707	3.46	1.85	41.5
14. Hood Support/Middle Hood(a)	0	65	68.1	87896	1422	4171	3702	3.34	1.86	45.3
15. Hood Support/Middle Hood(a)	0	-34.7	60.8	80662	1588	3708	3440	3.76	2.00	41.5

Note: (a) Full penetration weld so that weld factor, WF=1.4.

Table 4a. Limiting non-weld locations at MUR with frequency shifts. Stress ratios are grouped according to stress type (maximum – SR-P; or alternating – SR-a). Locations are depicted in Figure 3a-b.

Stress Ratio	Location	Location (in.)			node	Stress Intensity (psi)			Stress Ratio		% Freq. Shift	Dom. Freq. (Hz)
		x	y	z		Pm	Pm+Pb	S_{alt}	SR-P	SR-a		
SR-P	1. Outer portion of inner hood (top near closure plate)	109	-27.6	95.3	44886	6842	9587	1377	2.47	8.98	10	48.7
"	2. Bottom of inner hood	-110.8	38.4	10.2	41448	4875	4906	2882	3.47	4.29	10	48.2
"	3. Mid-height of inner hood	83.4	35.9	50.9	40188	3727	6843	6444	3.70	1.92	10	48.7
SR-a	1. Inner hood	83.4	35.9	50.9	40188	3727	6843	6444	3.70	1.92	10	48.7
"	2. Middle Hood	-25.6	68.9	35.1	37926	1612	5908	5598	4.29	2.21	2.5	47.5
"	3. Middle Hood	28.4	67.3	52.2	37238	1735	5853	5532	4.33	2.24	2.5	47.5
"	4. Middle Hood	-24.2	64.9	69	37916	1516	5936	5498	4.27	2.25	2.5	47.5
"	5. Inner Hood	84	37.2	37.7	40185	3291	5550	5262	4.57	2.35	10	48.7
"	6. Inner Hood	30.4	33.5	68.2	42011	1723	5542	5222	4.57	2.37	-2.5	48.6
"	7. Inner Hood	93.6	36	50.8	40554	3013	5436	5166	4.66	2.39	10	48.7
"	8. Inner Hood	-28.6	37.4	36.1	41834	1796	5456	5159	4.65	2.40	-2.5	48.6
"	9. Inner Hood	73.2	36	50.4	40518	2845	5387	5063	4.71	2.44	10	48.7

Table 4b. Limiting peak stress ratios, SR-P, on welds at MUR with frequency shifts. Locations are depicted in Figure 3c-e.

Location	Location (in.)				Stress Intensity (psi)			Stress Ratio		% Freq. Shift	Dom. Freq. (Hz)
	x	y	z	node	Pm	Pm+Pb	S_{alt}	SR-P	SR-a		
1. Skirt/Cap Strip/Skirt Ext	118.8	0.6	-2	88325	2951	11048	1996	1.26	3.44	-2.5	22.4
2. Closure Plate/Inner Hood	108.4	27.9	94.9	85409	6161	9041	2474	1.51	2.78	2.5	46.8
3. Bottom Skirt/Drain Channel	73.8	-93.1	-94.2	93833	2319	8247	5988	1.69	1.15	10	28.4
4. Inner Hood Support/Mid Cover Plate/Backing Bar	0	38.4	7.5	86960	5368	5418	3169	1.73	2.17	-10	48.6
5. Inner Hood Support/Vane Bank/Mid Cover Plate	0	22.9	7.5	93159	5264	5299	3949	1.77	1.74	10	36.8
6. Drain Pipe/Skirt	88.2	79.6	-20.5	91083	2718	7665	2284	1.82	3.01	10	48.7
7. KT1-444/Inner Hood	109.8	-38.4	9.5	92106	5027	5028	2549	1.85	2.69	10	48.6
8. Bottom Skirt/Drain Channel	-118.2	-12	-94.2	93758	2266	7416	4925	1.88	1.39	5	47.3
9. Side Vane Bank/Mid Cover Plate	118.8	-14.4	7.5	86577	4888	6763	1198	1.90	5.74	5	46.3
10. Middle Side Panel/Top Cover/Top Perf. Plate/ Closure Plate	-108.4	45.9	95.9	85891	4706	5397	1526	1.98	4.50	10	36.8

Table 4c. Limiting 21 alternating stress ratios, SR-a, on welds at MUR with frequency shifts. Locations are depicted in Figure 3f-h.

Location	Location (in.)				Stress Intensity (psi)			Stress Ratio		% Freq. Shift	Dom. Freq. (Hz)
	x	y	z	node	Pm	Pm+Pb	S_{alt}	SR-P	SR-a		
1. Backing Bar/Middle Hood	-29.1	69.9	8.5	87919	923	6983	6566	2.00	1.05	2.5	47.7
2. Backing Bar/Inner Hood	30	38.4	8.5	88060	1258	6630	6194	2.10	1.11	-2.5	48.6
3. Hood Support/Inner Hood(a)	0	-36.1	49.6	80664	2793	6558	6148	2.13	1.12	10	36.8
4. Drain Channel/Bottom of Skirt	73.8	-93.1	-94.2	93833	2319	8247	5988	1.69	1.15	10	28.4
5. Hood Support/Inner Hood(a)	0	37.2	38.4	88025	2613	6510	5978	2.14	1.15	10	36.8
6. Hood Support/Inner Hood(a)	0	34.7	60.8	88019	2545	6161	5744	2.26	1.20	10	36.8
7. Drain Channel/Bottom of Skirt	-118.2	12	-94.2	82775	2636	6037	5677	2.31	1.21	10	47.7
8. Backing Bar/Inner Hood	81.9	38.4	8.5	85261	1367	5470	5131	2.55	1.34	10	48.7
9. Backing Bar/Middle Hood	-16.5	69.9	8.5	87922	1408	5401	4997	2.58	1.37	2.5	47.7
10. Hood Support/Middle Hood(a)	0	68.3	42.2	87903	2143	5420	4917	2.57	1.40	-5	47.7
11. Hood Support/Inner Hood(a)	59.5	36.1	49.6	88043	2131	5250	4909	2.66	1.40	10	36.8
12. Hood Support/Middle Hood(a)	0	67.1	53.3	87900	2342	5115	4705	2.73	1.46	7.5	41.8
13. Backing Bar/Inner Hood	17.2	38.4	8.5	88057	1584	4968	4609	2.81	1.49	-2.5	48.6
14. Backing Bar/Inner Hood	42.7	38.4	8.5	88063	1891	4952	4605	2.82	1.49	-2.5	48.6
15. Hood Support/Inner Hood(a)	59.5	37.2	38.4	88046	2061	4906	4573	2.84	1.50	10	36.8
16. Hood Support/Middle Hood(a)	0	65.6	64.4	87897	2017	4893	4534	2.85	1.51	-5	47.7
17. Hood Support/Inner Hood(a)	0	37.9	27.2	88028	2022	4905	4515	2.84	1.52	10	36.8
18. Hood Support/Inner Hood(a)	0	32.9	71.9	88016	1927	4690	4429	2.97	1.55	10	36.8
19. Hood Support/Inner Hood(a)	59.5	34.7	60.8	88040	2006	4690	4319	2.97	1.59	10	36.8
20. Backing Bar/Middle Hood	42.1	69.9	8.5	87826	1637	4384	4152	3.18	1.65	2.5	47.7
21. Backing Bar/Inner Hood	-94.8	38.4	8.5	85455	2734	4351	4012	3.20	1.71	10	48.6

Note: (a) Full penetration weld so that weld factor, WF=1.4.

Table 4d. Remaining nodes on welds with alternating stress ratios, SR-a, on welds below 2.0 at MUR conditions with frequency shifts. Locations are depicted in Figure 3f-h.

Location	Location (in.)				Stress Intensity (psi)			Stress Ratio		% Freq. Shift	Dom. Freq. (Hz)
	x	y	z	node	Pm	Pm+Pb	S_{alt}	SR-P	SR-a		
22. Hood Support/Vane Bank/Mid Cover Plate	0	22.9	7.5	93159	5264	5299	3949	1.77	1.74	10	36.8
23. Outlet Plenum/Inner Hood	108.4	35.9	51.5	85304	1737	4285	3938	3.25	1.74	10	48.7
24. Hood Support/Middle Hood[(a)]	0	69.2	31	87906	1718	4240	3855	3.29	1.78	-5	47.7
25. Backing Bar/Inner Hood	68.6	38.4	8.5	85256	3216	4014	3786	2.89	1.81	10	48.7
26. Hood Support/Inner Hood[(a)]	59.5	37.9	27.2	88049	1827	4005	3776	3.48	1.82	10	36.8
27. Hood Support/Middle Hood[(a)]	54.5	67.1	53.3	87806	1211	3919	3548	3.56	1.94	10	46.8
28. Hood Support/Middle Hood[(a)]	0	69.7	19.7	87909	1119	3653	3460	3.82	1.99	2.5	47.7

Note: (a) Full penetration weld so that weld factor, WF=1.4.

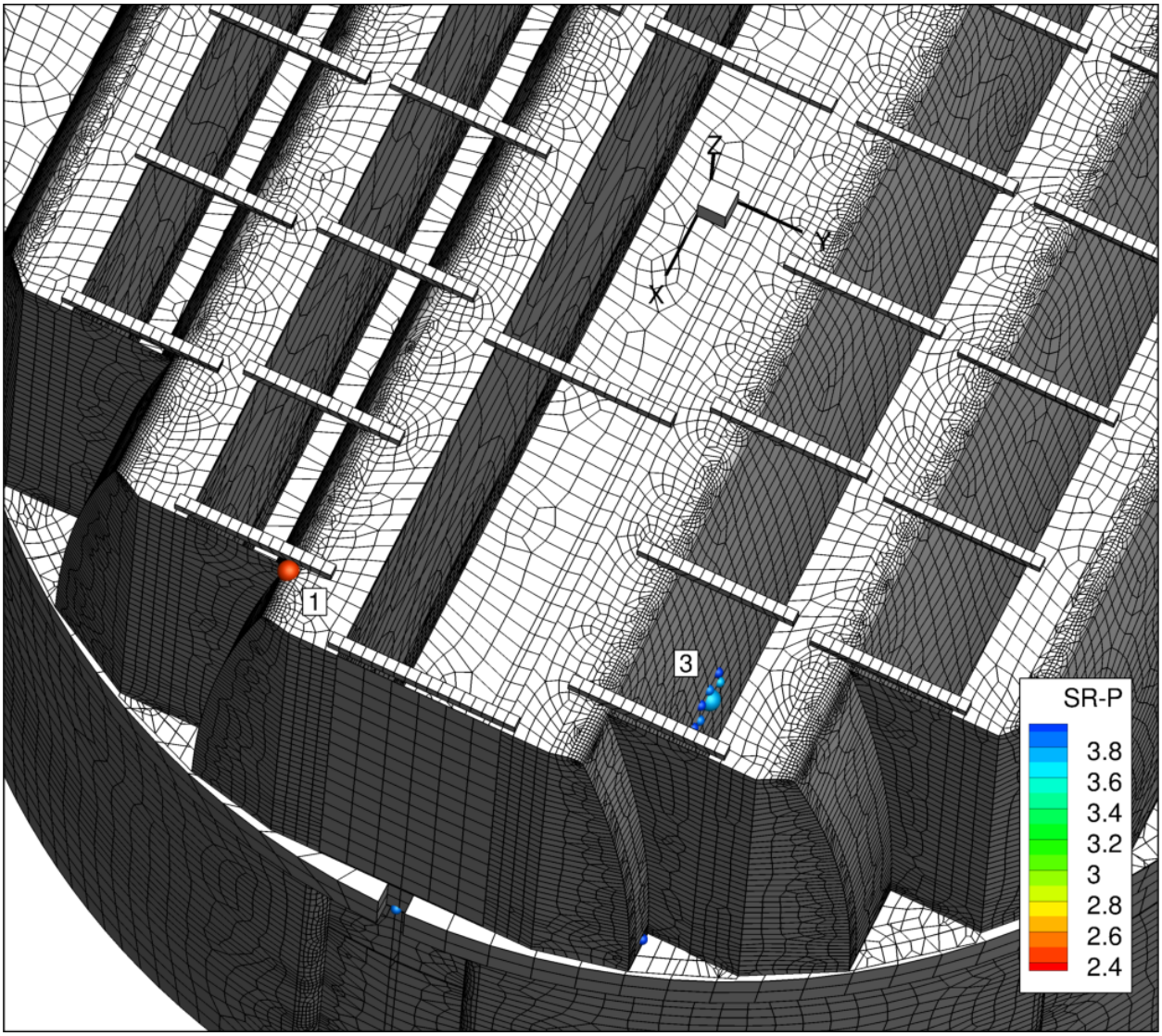

Figure 3a. Locations of m inimum stress ratios, SR-P ≤4, associated with m aximum stress intensities at non-welds for MUR with frequenc y shifts. The recorded stress ratio is the minimum value taken over all frequency shifts. The number refer to the enumerated location for SR-P values at non-welds in Table 4a. This view shows location 1 and 3.

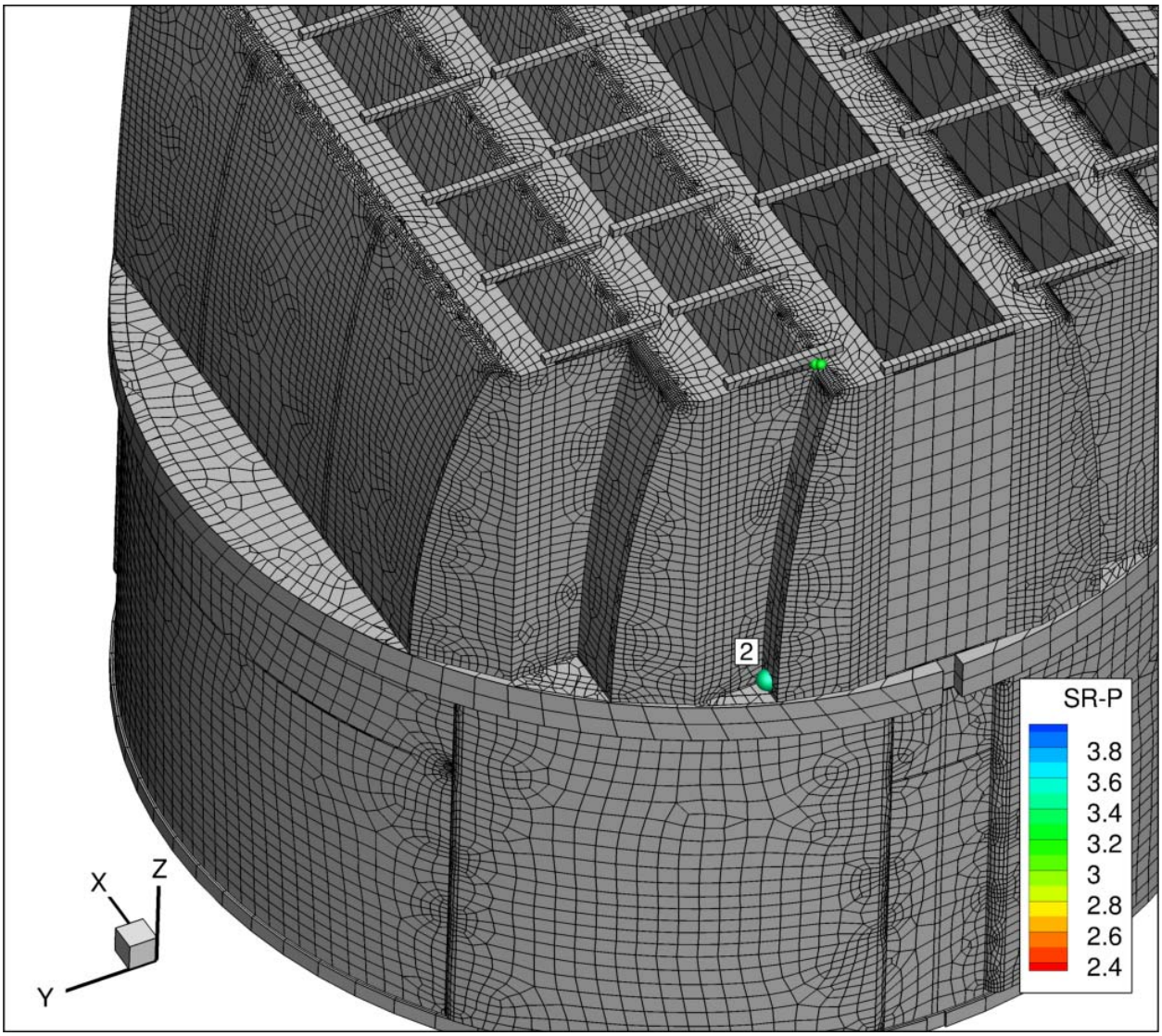

Figure 3b. Locations of minimum stress ratios, SR-P ≤4, associated with maximum stress intensities at non-welds for MUR operation with frequency shifts. The recorded stress ratio is the minimum value taken over all frequency shifts. Numbers refer to the enumerated locations for SR-a values at non-welds in Table 4a. This view shows location 2.

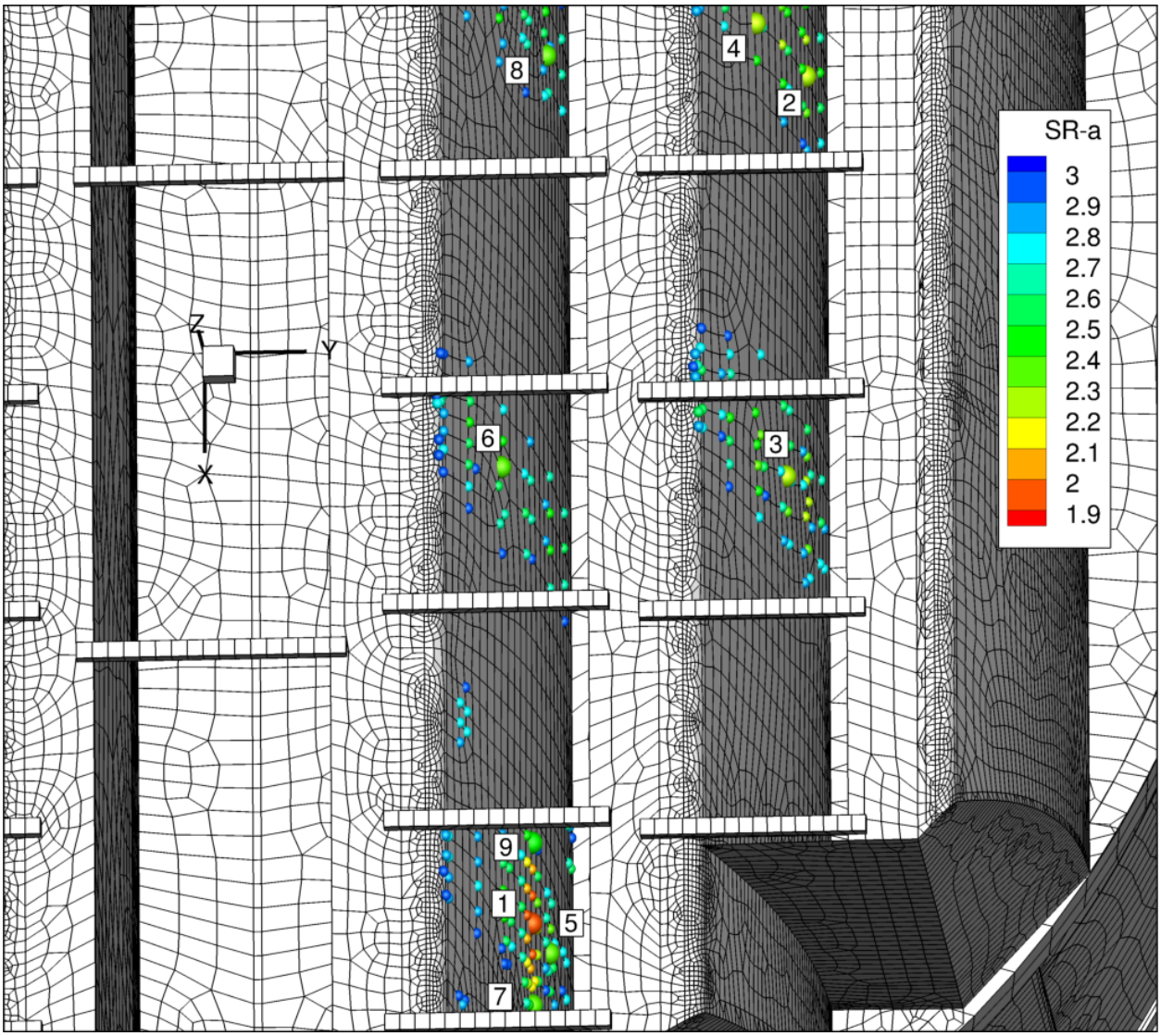

Figure 3c. Locations of m inimum alternating stress ratios, SR-a ≤3, at non-welds for MUR operation with frequency shifts. The recorded st ress ratio at a node is the m inimum value taken over all frequency shifts. Numbers refer to the enumerated locations for SR-P values at welds in in Table 4a. All locations 1-9 are shown.

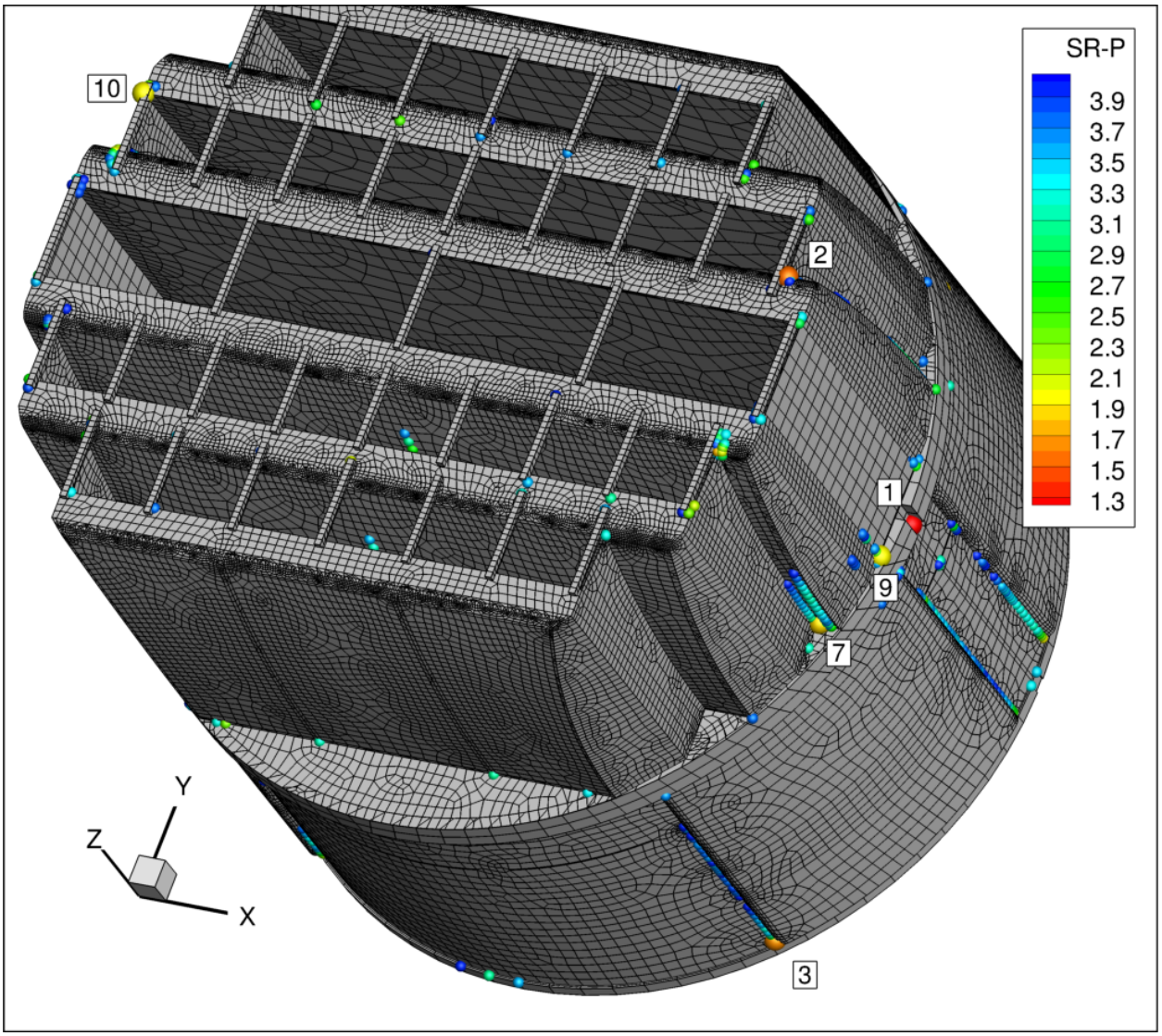

Figure 3d. Locations of m inimum stress ratios, SR-P ≤4, associated with m aximum stress intensities at welds for MUR with frequency shifts. The recorded stress ratio at a node is the minimum value taken over all frequency shifts. Numbers refer to the en umerated locations for SR-P values at welds in in Table 4b. This view shows locations 1-3, 7, 9 and 10.

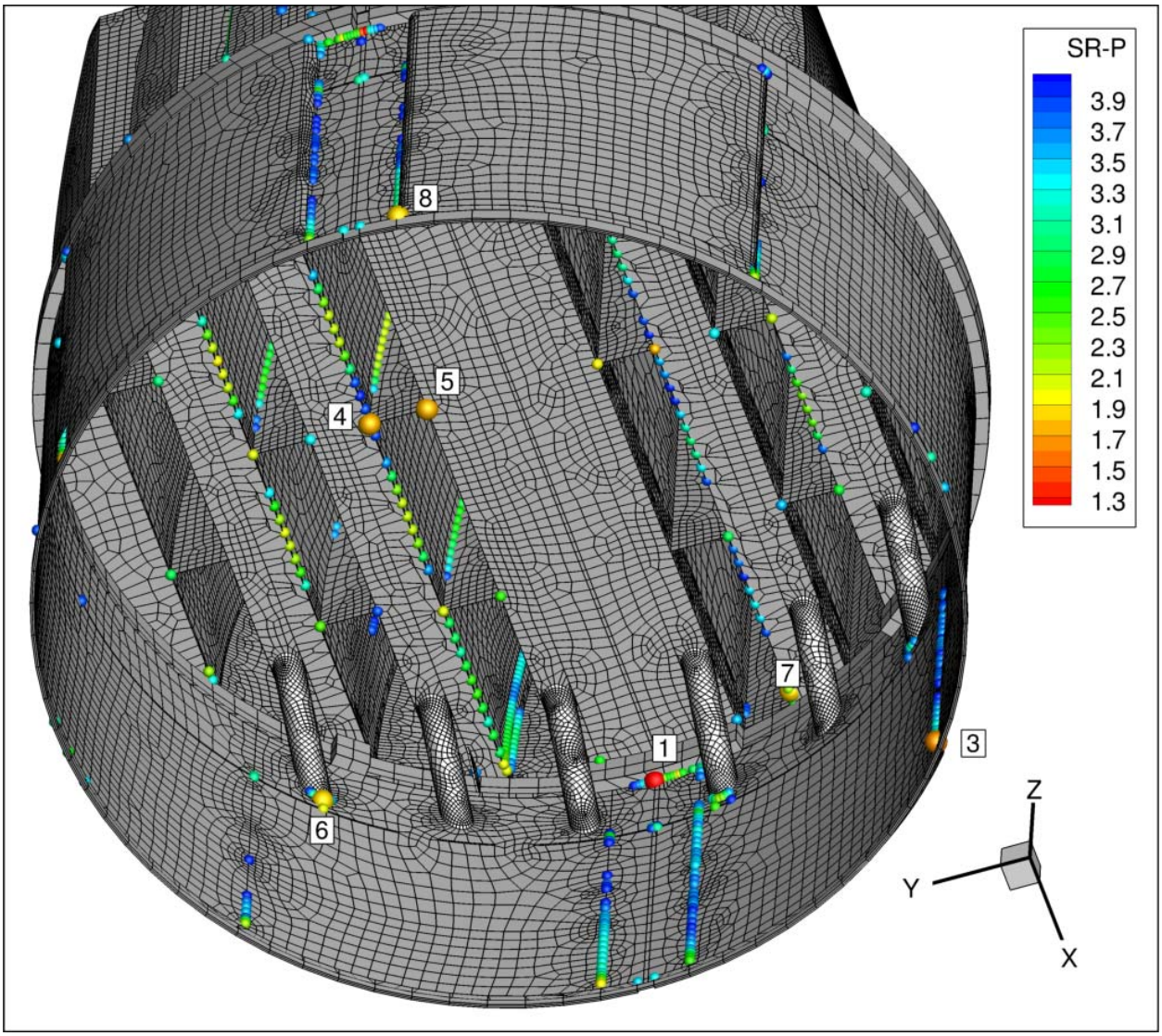

Figure 3e. Locations of m inimum stress ratios, SR-P ≤4, associated with m aximum stress intensities at welds for MUR with frequency shifts. The recorded stress ratio at a node is the minimum value taken over all frequency shifts. Numbers refer to the en umerated locations for SR-P values at welds in in Table 4b. This view shows locations 1, and 3-8.

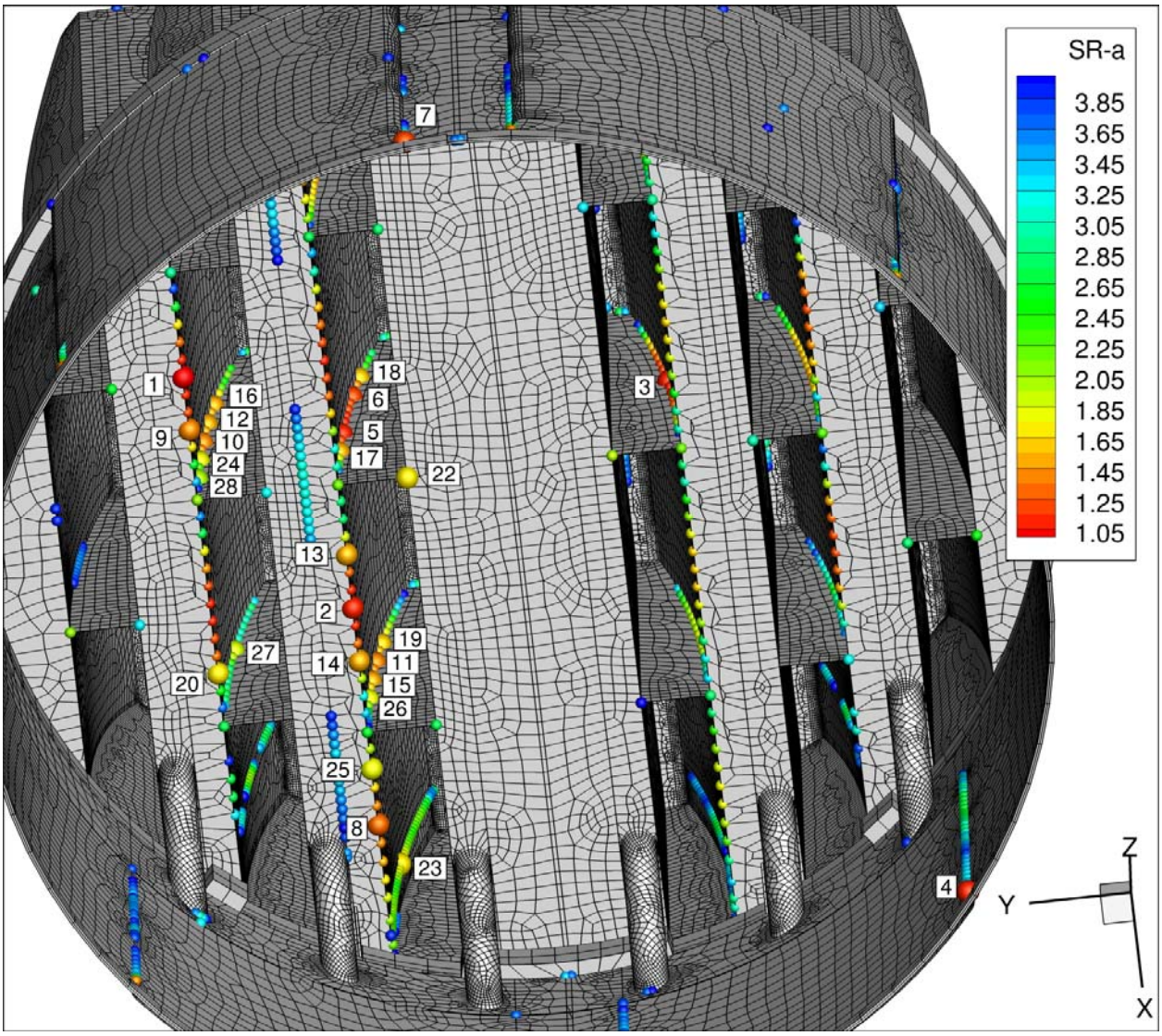

Figure 3f. Locations of minimum alternating stress ratios, SR-a≤4, at welds for MUR with frequency shifts. The recorded stress ratio at a node is the minimum value taken over all frequency shifts. Numbers refer to the enumerated locations for SR-a values at welds in Table 4c-d. Locations 1-20 and 22-28 are shown

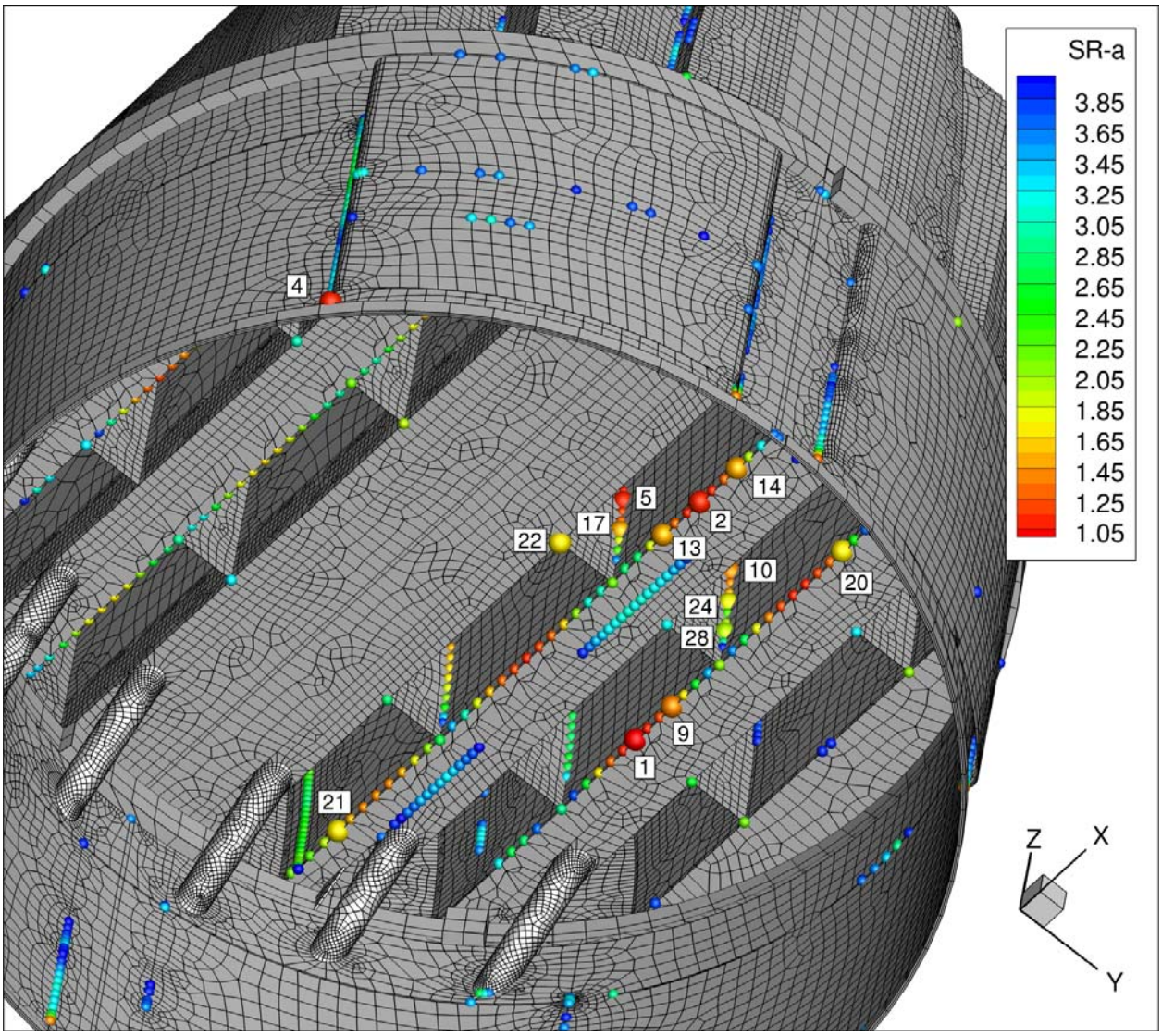

Figure 3g. **Locations of minimum alternating stress ratios, SR-a ≤4, at welds for MUR with frequency shifts. The recorded stress ratio at a node is the minimum value taken over all frequency shifts. Numbers refer to the enumerated locations for SR-a values at welds in Table 4c-d. Second view showing locations 1, 2, 4, 5, 9, 10, 13, 14, 17, 20-22, 24 and 28.

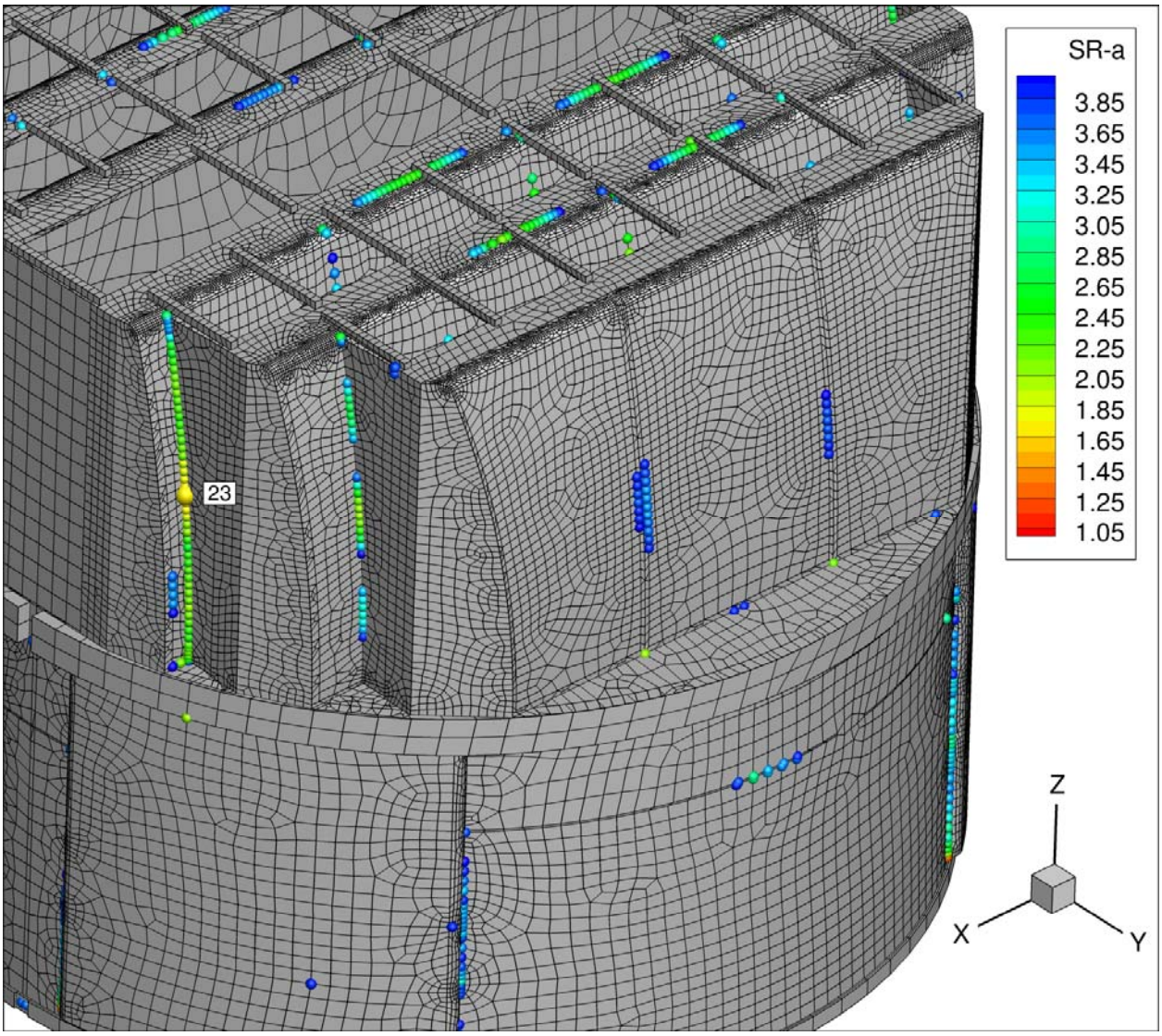

Figure 3h. Locations of minimum alternating stress ratios, SR-a≤4, at welds for with frequency shifts. The recorded stress ratio at a node is th e minimum value taken over all frequency shifts. Numbers refer to the en umerated locations for SR-a values at welds in Table 4c-d. Third view showing location 23.

2.3 Frequency Content and Sensitivity to Frequency Shift of the Stress Signals

The spectral content in the stress response is examined by presenting the PSD and accumulative PSDs of selected nodes and stress components. The accumulative PSDs are computed directly from the Fourier coefficients as

$$\Sigma(\omega_n) = \sqrt{\sum_{k=1}^{n} \left|\tilde{\sigma}(\omega_k)\right|^2}$$

where $\tilde{\sigma}(\omega_k)$ is the complex stress harmonic at frequency, ω_k. Accumulative PSD plots are useful for determining the frequency components and frequency ranges that make the largest contributions to the fluctuating stress. Unlike PSD plots, no "binning" or smoothing of frequency components is needed to obtain smooth curves. Steep step-like rises in $\Sigma(\omega)$ indicate the presence of a strong component at a discrete frequency whereas gradual increases in the curve imply significant content over a broader frequency range. From Parsival's theorem, equality between $\Sigma(\omega_N)$ (where N is the total number of frequency components) and the RMS of the stress signal in the time domain is established.

The accumulative PSD and PSDs are examined at five nodes each one representative of a weld configuration (a)-(e) as described in Section 5.2. These nodes are listed in Table 5.

Table 5. List of nodes selected for plotting stress PSDs in Figure 4.

Location	Entry in Table 4c, d	Node	SR-a.	Dom. Freq.	PSDs
Backing Bar/Middle Hood	1	87919	1.05	47.7	Figure 4a
Hood Support/Inner Hood	3	80664	1.12	36.8	Figure 4b
Bottom Skirt/Drain Channel	4	93833	1.15	28.4	Figure 4c
Hood Support/Vane Bank/Mid Cover Plate	22	93159	1.74	36.8	Figure 4d
Closure Plate/Inner Hood	23	85304	1.74	48.7	Figure 4e

In each case, since there are six stress components and up to three different section locations for shells (the top, mid and bottom surfaces), there are a total of 18 stress histories per component. Moreover, at junctions there are at least two components that meet at the junction. The particular stress component that is plotted is chosen as follows. First, the component and section location (top/mid/bottom) is taken as the one that has the highest alternating stress. This narrows the selection to six components. Of these, the component having the highest Root Mean Square (RMS) is selected.

The accumulative PSD and PSD curves are presented in Figure 4. The stress response at the limiting node (87919) is characterized by a single distinct peak about 47.7 Hz. This peak does not shift significantly with frequency shift, which is indicative of a structural mode being excited by a relatively broad acoustic peak. For the second location (80664) two peaks are present at

approximately 37 Hz and 48 Hz; frequency shifting amplifies the former peak to become dominant. The third location has a much richer spectrum reflecting the fact that the skirt contains many modes in the 0-200 Hz range. The fourth location (node 85304) is similar to the first location in that it contains a single dominant peak, here at approximately 52 Hz which corresponds to a structural mode that is excited when the 48.7 Hz peak in the load is shifted upward by +10%. Finally, the fifth node 93159 exhibits two peaks, again involving primarily the signal peaks at 36.8 Hz and 47.7-48.7 Hz.

From Table 4c-d it is evident that these are two peak frequencies dominate most of the stress response. The prevalence of these frequencies can also be visualized by plotting the dominant frequency over the dryer surface. Thus, for each finite element node the frequency associated with the largest stress harmonic (at any frequency shift) is recorded. As in Table 4 and Table 5, the pre-shift frequency is used. A contour map of this dominant frequency is shown in Figure 5 and provides a qualitative view of which dryer components appear most responsive to particular frequencies. Low frequency responses in the range 30-50 Hz dominate the inner and middle hoods, vane bank side plates, hood supports, and a large portion of the skirt. Over the 50-150 Hz range only the outer hoods exhibit a significant response, though these stresses are much lower than those at frequencies below 50 Hz.

Overall, the frequency responses and dominant frequency distributions are very similar to the ones in [3], which is expected since the applied signals are essentially identical (the scaling used to infer MUR from CLTP does not alter the frequency content other than the velocity square scaling of the amplitudes) and the PPD influence is limited to the vicinity of the perforated plates.

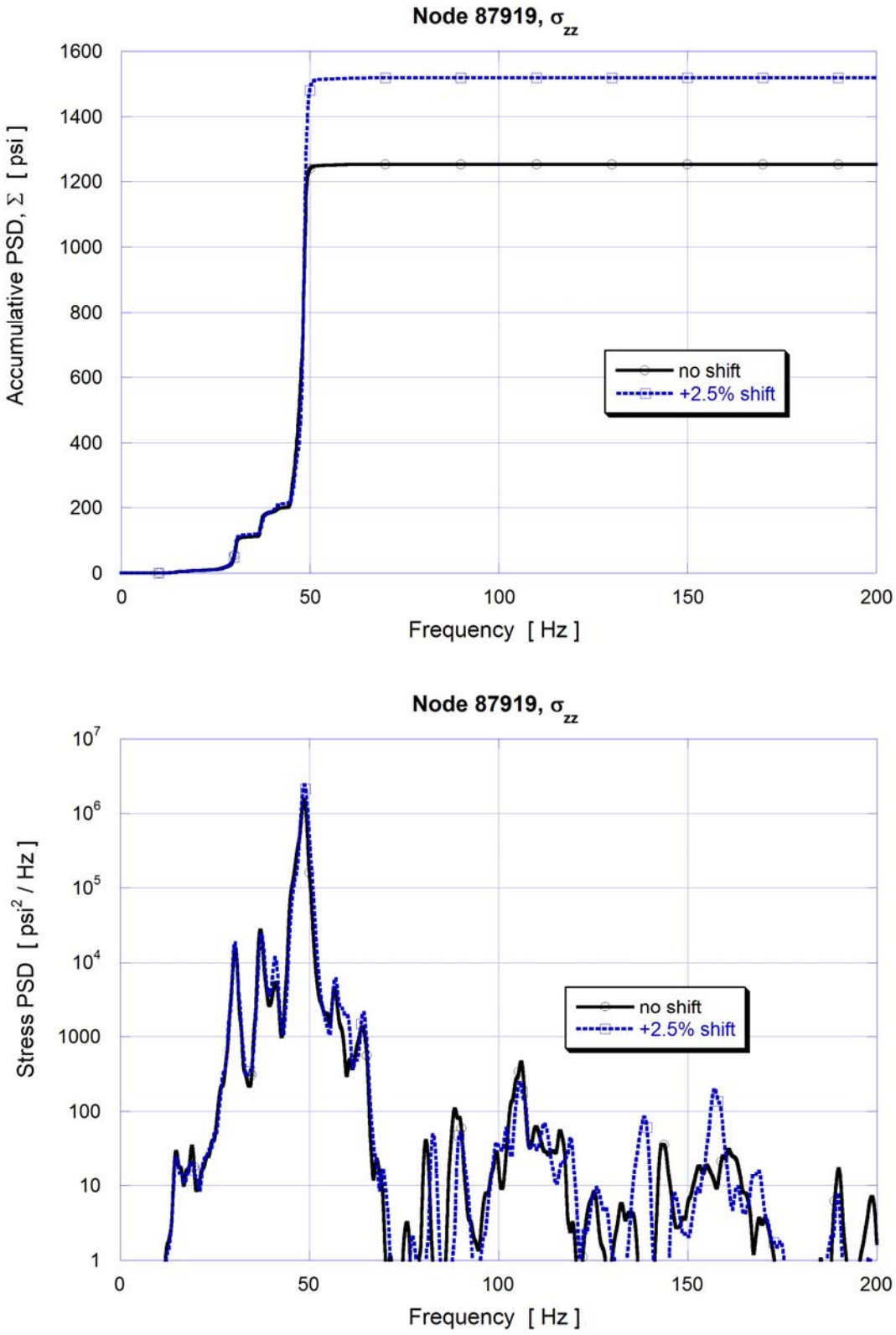

Figure 4a. Accumulative PSD and PSD curves of the σ_{zz} stress response at node 87919 at MUR operation.

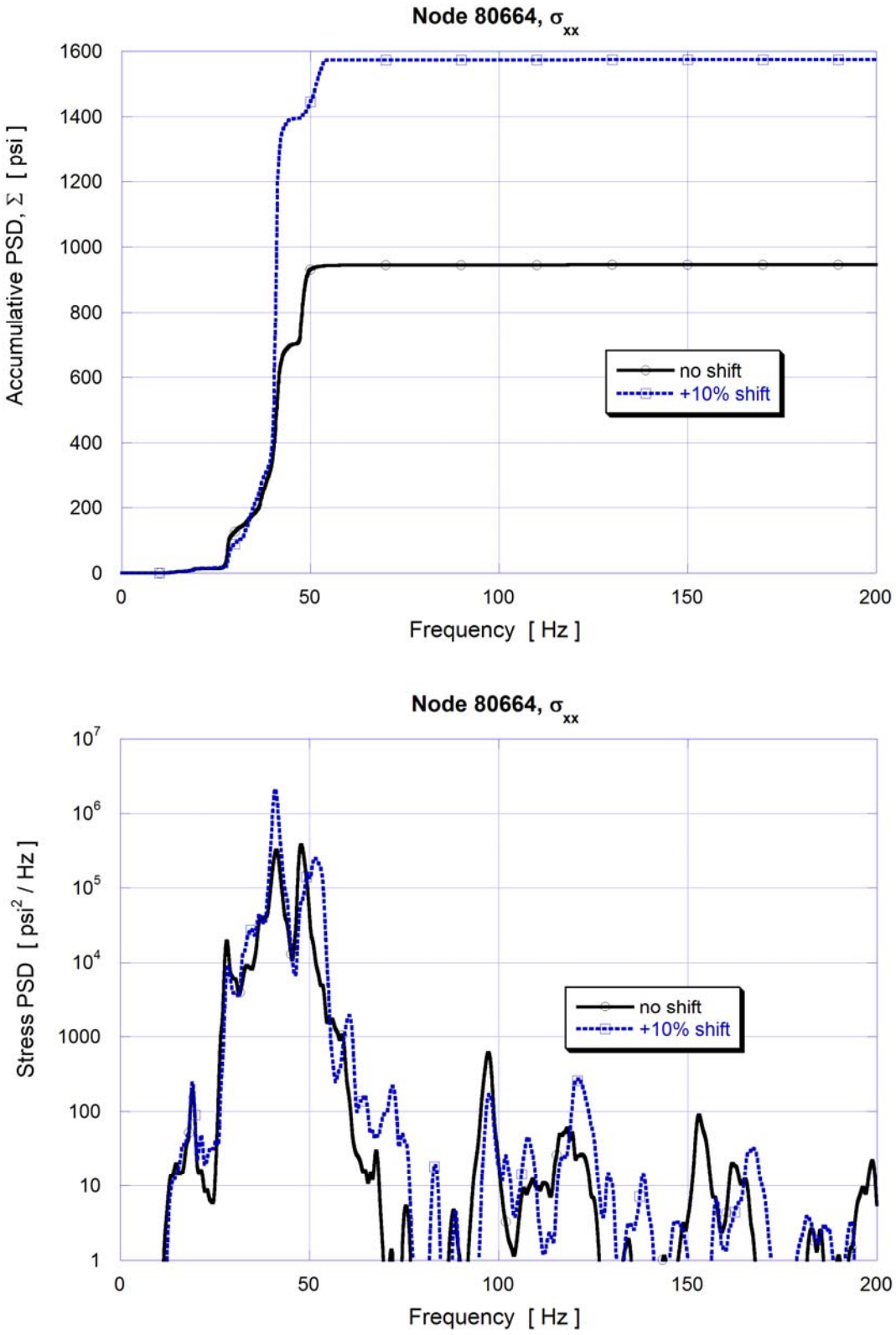

Figure 4b. Accumulative PSD and PSD curves of the σ_{xx} stress response at node 80664 at MUR operation

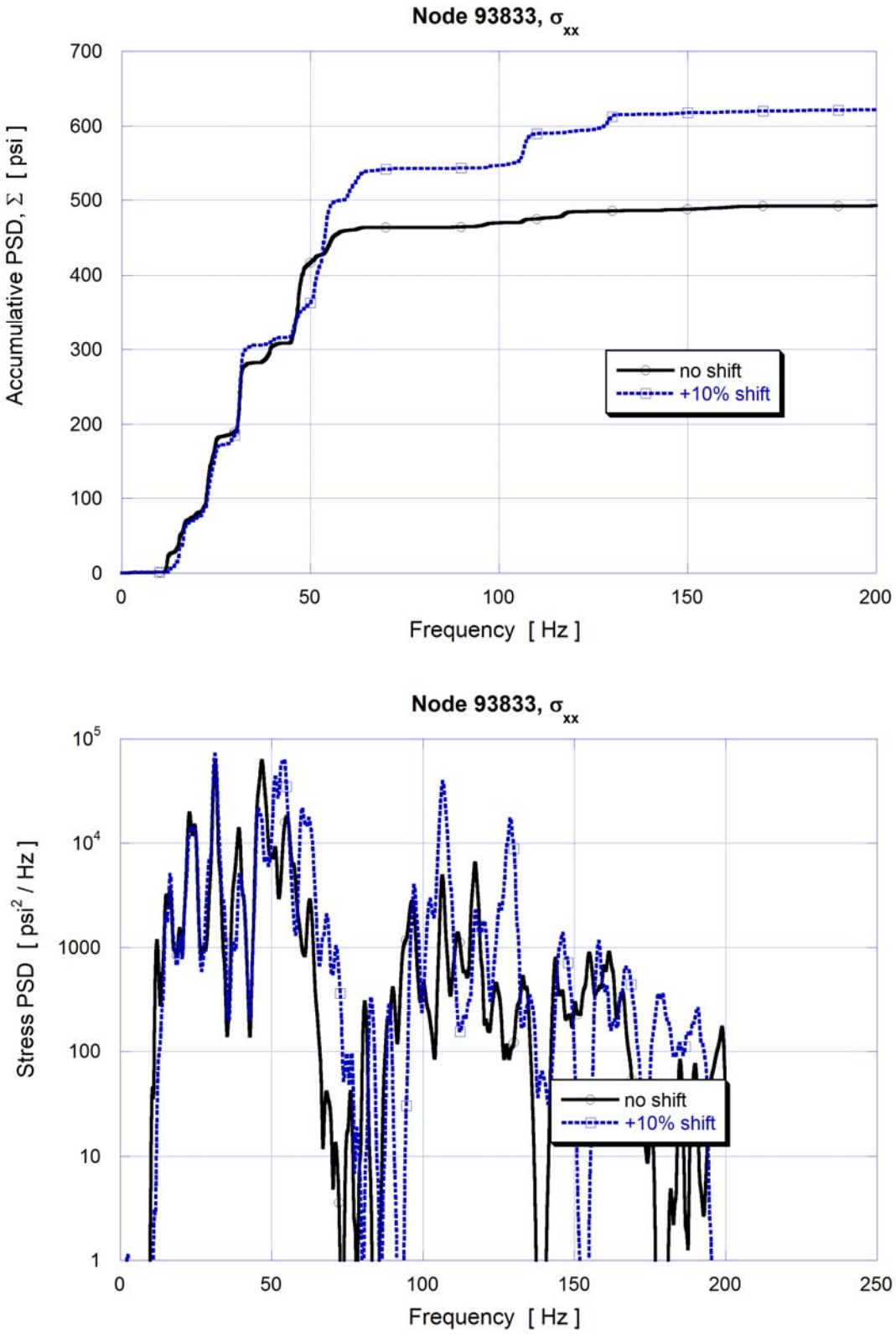

Figure 4c. Accumulative PSD and PSD curves of the σ_{xx} stress response at node 93833 at MUR operation.

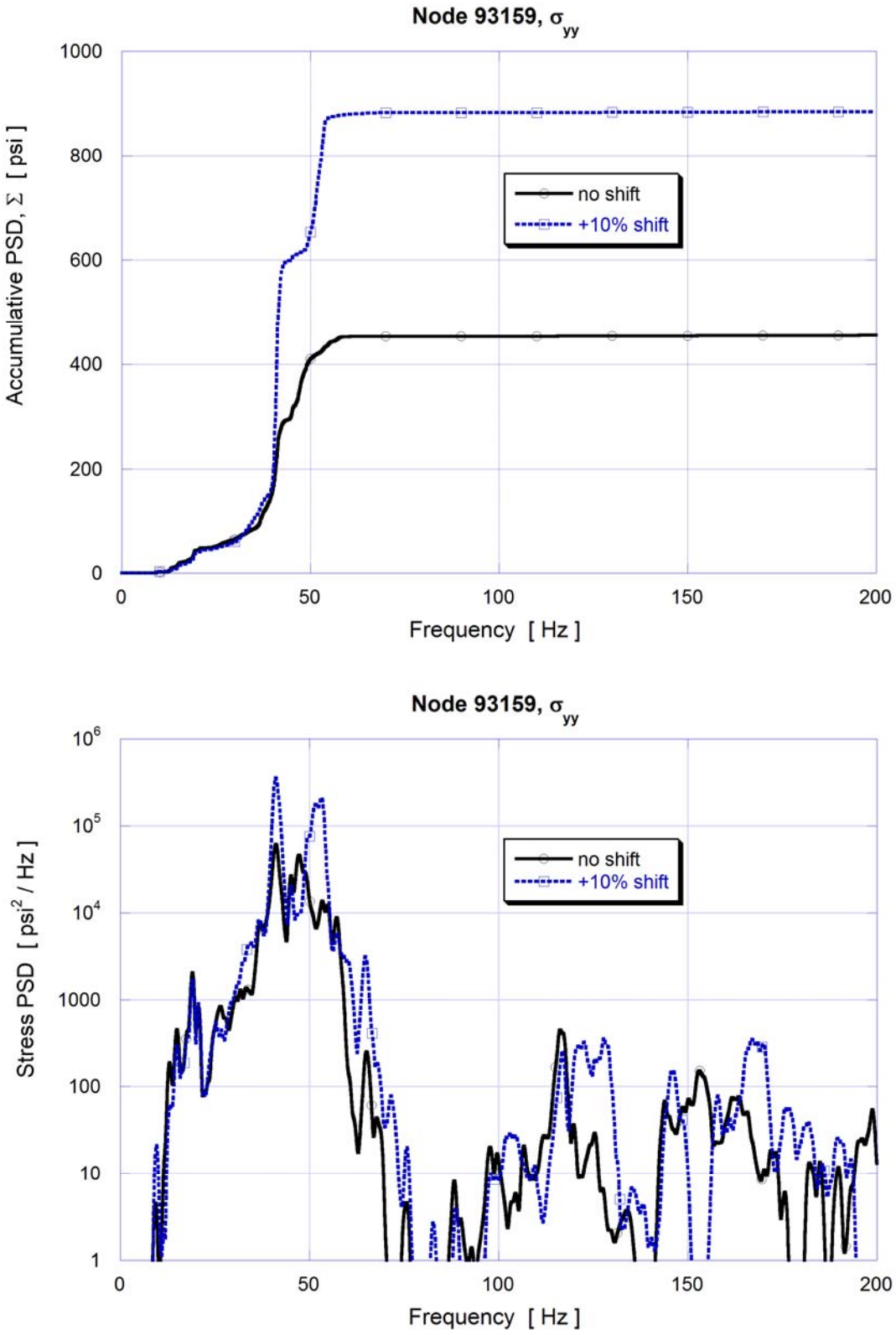

Figure 4d. Accumulative PSD and PSD curves of the σ_{yy} stress response at node 93159 at MUR operation.

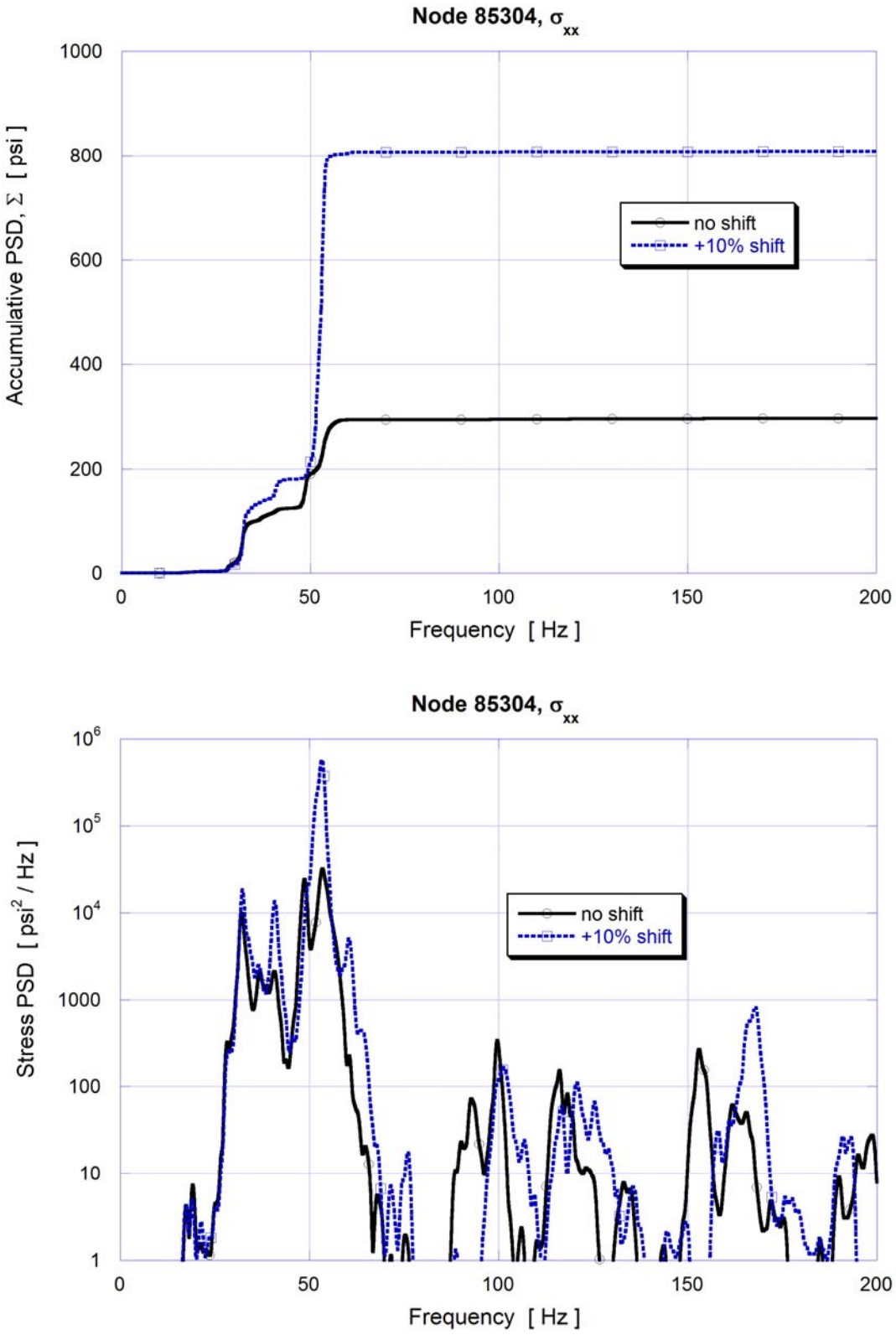

Figure 4e. Accumulative PSD and PSD curves of the σ_{xx} stress response at node 85304 at MUR operation.

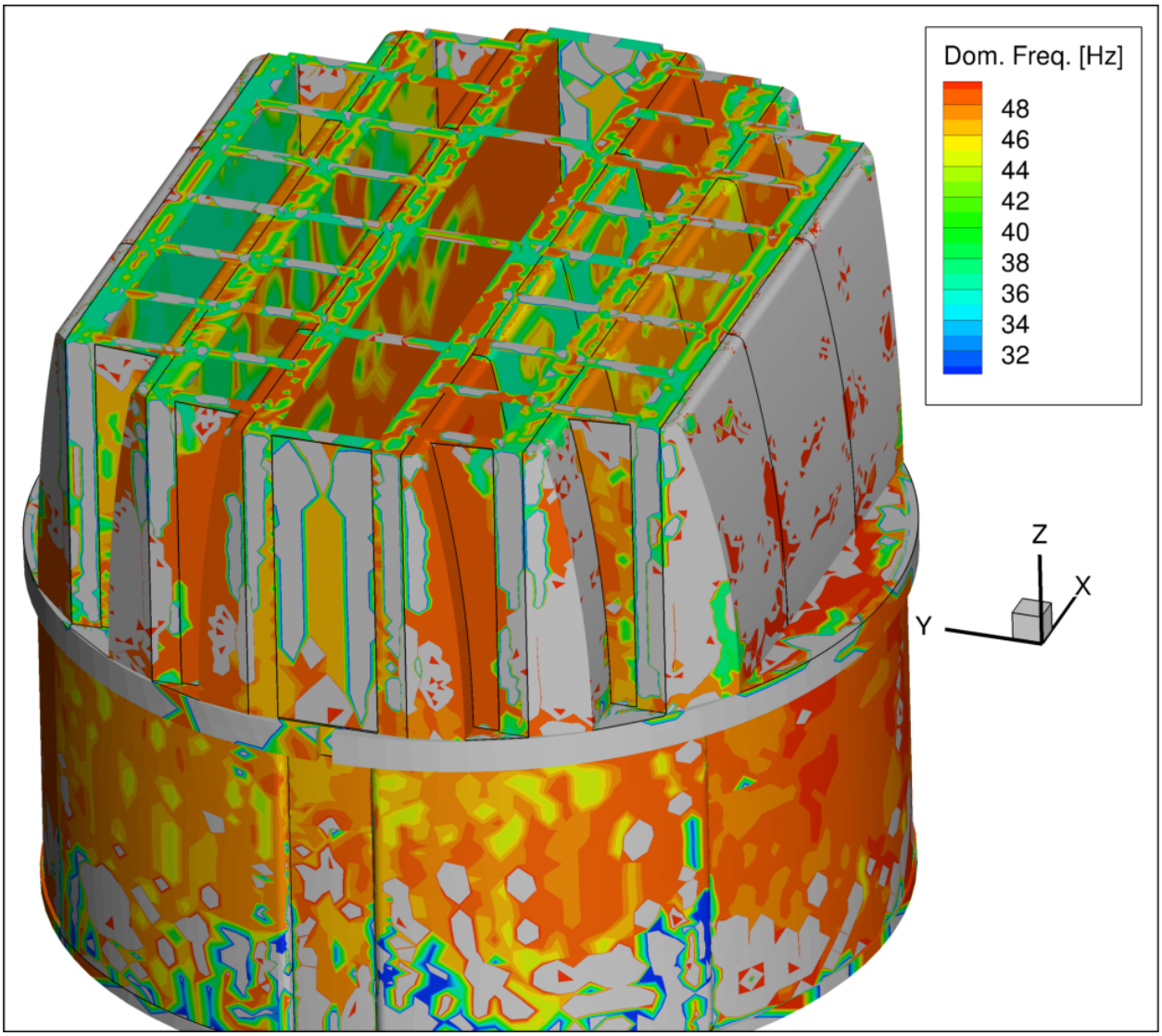

Figure 5a. Contour map showing the dominant frequencies (i.e., the frequency with the largest stress harmonic). This shows locations with dominant frequencies in the range 30-50 Hz.

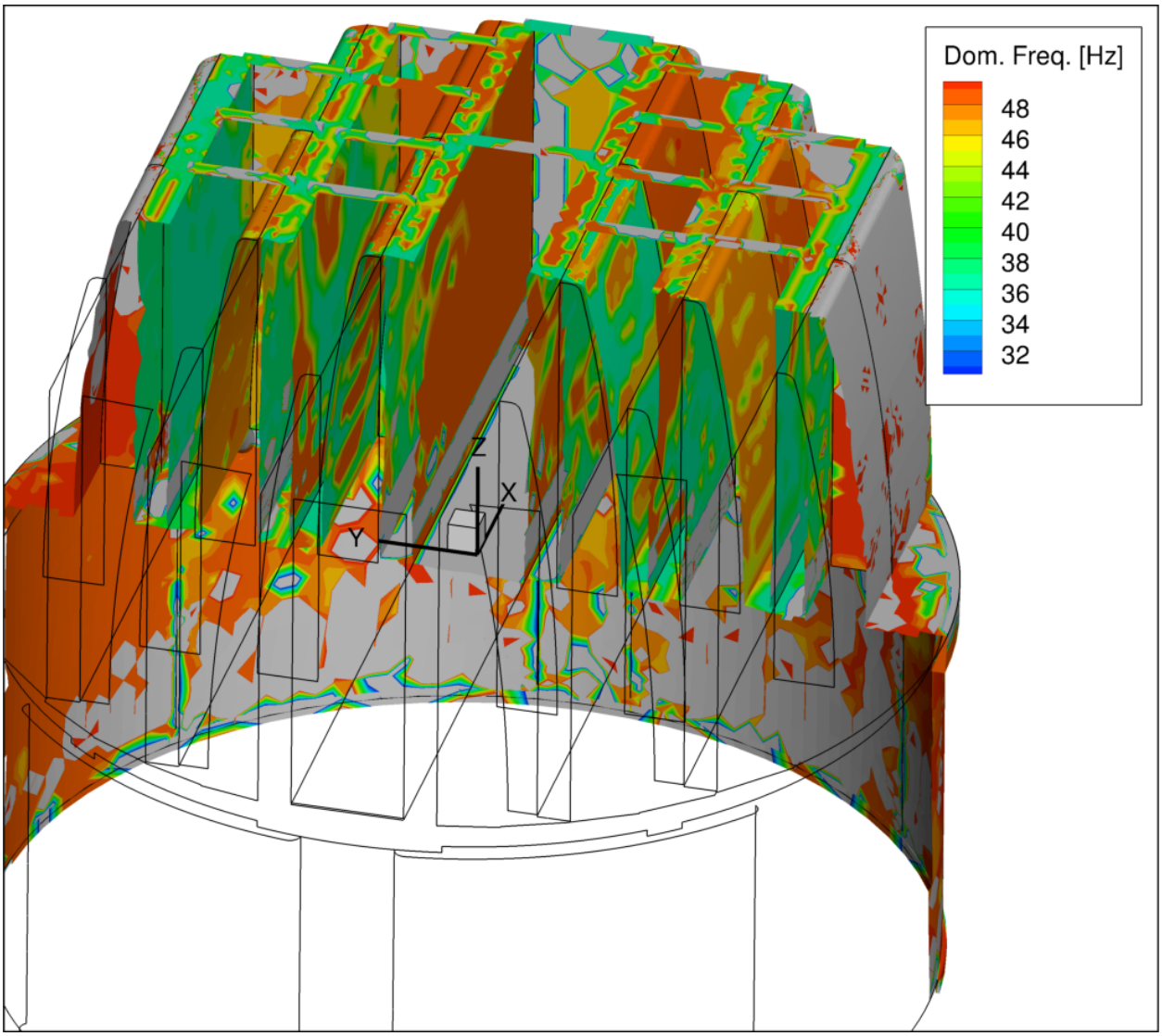

Figure 5b. Contour map showing the dominant frequencies (i.e., the frequency with the largest stress harmonic). This second view shows locations with dominant frequencies in the range 30-50 Hz exposing more of the inner and middle hood structures.

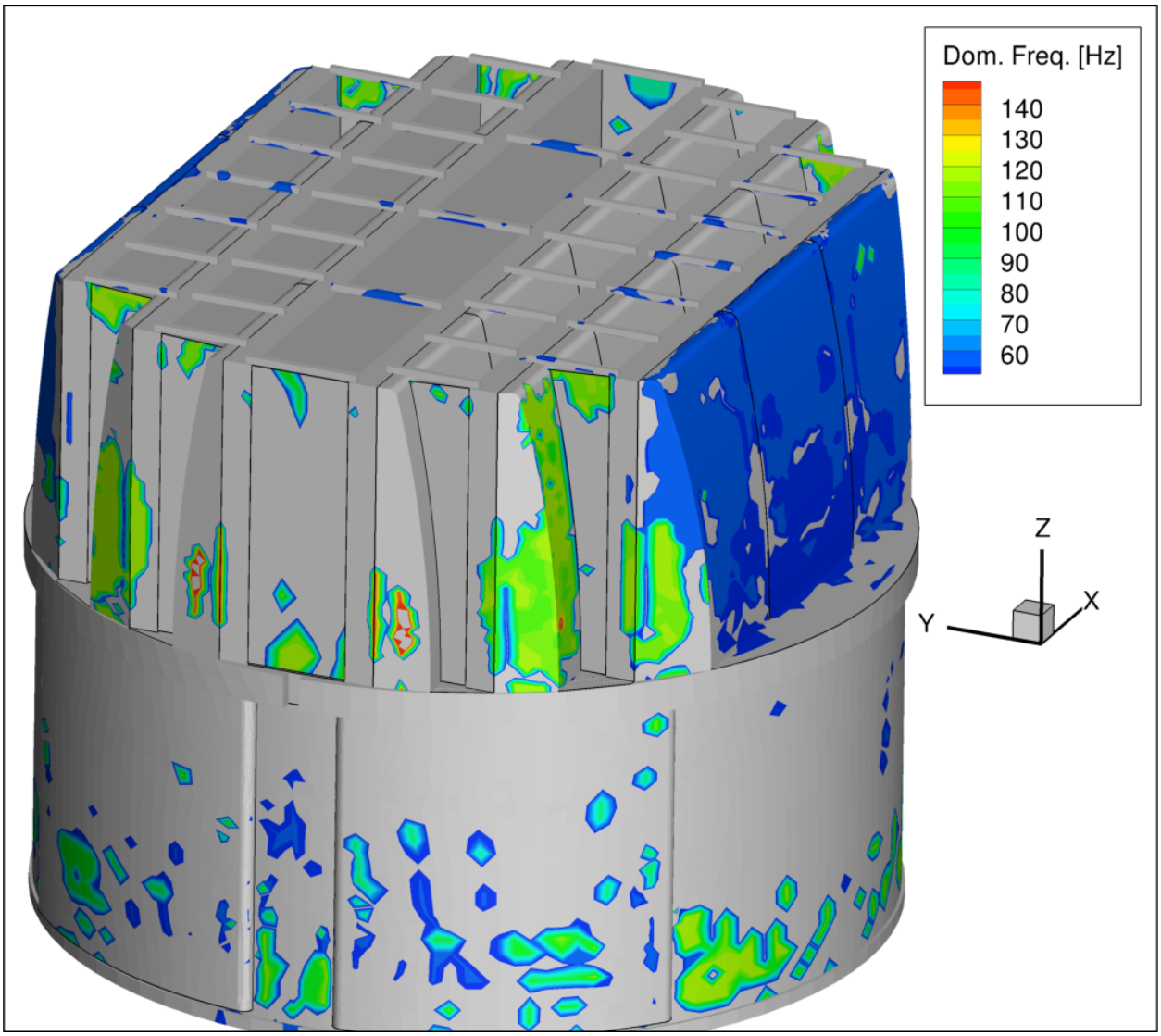

Figure 5c. Contour m ap showing the dominant frequencies (i.e., the frequency with the largest stress harmonic). This plot shows locations with dominant frequencies in the range 50-150 Hz.

3. Comparison of Stresses With and Without PPD

In order to assess the relative significance of PPD upon the steam dryer response, the results obtained here at MUR conditions with PPD are compared against those acquired without PPD. The latter results are obtained using the real time stress evaluation capability in the harmonic stress analysis software which allows the stresses to be calculated at selected locations on the dryer. Here the limiting locations identified at MUR with PPD are reprocessed using the same MUR signals, but the FEA model without VIL (i.e., as used in CDI Report 15-06, [3]).

Table 6 compares the stress ratios obtained with and without PPD at MUR operation. The limiting location experiences a 1.2% stress reduction which increases the stress ratio from 1.04 to 1.05. Stress reductions in the vicinity of perforated plates are generally in the 1-2% range; further away at the drain channels the changes are smaller as expected.

Overall, the reductions in stress at the limiting locations are smaller than desired. The influence of PPD on stress near the perforated plates depends on several factors including: relative thicknesses of the affected parts, mode shapes, frequency (higher frequency modes are less affected by PPD), and how well an acoustic mode couples into the structure. Modes that involve significant perforated plate motion generally experience the strongest reduction, particularly if the modal mass contribution from the perforated plates is a significant fraction of the total modal mass for that mode. Estimating the relative contribution of PPD to a particular node near the perforated plates is generally not possible *a priori* other than: (i) the expectation that nodes far away from the perforated plates should experience a negligible change in stress; and (ii) past experience with PPD damping for nodes near the perforated plates indicates stress reductions in the approximate range of 0 to 10%. Outliers with larger stress reductions are possible as are stress increases in some cases, typically ones where the stresses are displacement rather than force driven.

Figure 6 shows the stress changes due to PPD for all nodes on the dryer with SR-a<5 (at MUR) excluding the perforated plates themselves. This plot concurs with prior experience in using PPD. Up to 23% stress reduction is observed for isolated locations; however, for SR-a<3 the largest reduction is 3.7%. Some stress increases are observed reflecting the expected behavior when a stress is displacement driven, meaning that the stress results mainly from the response induced by more distant loads than from local loads (e.g., the global dryer response due to loads on the outer hoods). The distribution of the stress change over the dryer is depicted in Figure 7 which shows that, as expected, the main stress reductions occur on the perforated plates and attached structures. The view from underneath the dryer (Figure 7b) reveals that the bottoms of the hood supports do experience reductions of approximately 3% in some cases, but not in the limiting locations. For example, the middle hood/cover plate/backing bar junction (entry 10, node 87903) experiences a stress reduction of 2.6%. However, SR-a=1.40 so this reduction is not at the location where it is most needed.

In a summary sense, the overall PPD effect is within expectations, albeit somewhat weaker than experienced at some other plants. While the stresses at the limiting locations are reduced, these locations continue to be limiting.

Table 6. Comparison of stress ratios computed at MUR with and without PPD

Location	node	No PPD		With PPD		R_{PPD} (1)
		SR-P	SR-a	SR-P	SR-a	%
1. Backing Bar/Middle Hood	87919	1.98	1.04	2.00	1.05	-1.2
2. Backing Bar/Inner Hood	88060	2.09	1.10	2.10	1.11	-0.7
3. Hood Support/Inner Hood	80664	2.12	1.11	2.13	1.12	-0.5
4. Drain Channel/ Bottom of Skirt	93833	1.69	1.15	1.69	1.15	-0.1
5. Hood Support/Inner Hood	88025	2.14	1.14	2.14	1.15	-0.8
6. Hood Support/Inner Hood	88019	2.24	1.19	2.26	1.20	-0.9
7. Drain Channel/Bottom of Skirt	82775	2.32	1.21	2.31	1.21	0.3
8. Backing Bar/Inner Hood	85261	2.55	1.34	2.55	1.34	-0.3
9. Backing Bar/Middle Hood	87922	2.55	1.36	2.58	1.37	-0.4
10. Hood Support/Middle Hood	87903	2.51	1.36	2.57	1.40	-2.6
11. Hood Support/Inner Hood	88043	2.65	1.40	2.66	1.40	-0.2
12. Hood Support/Middle Hood	87900	2.69	1.44	2.73	1.46	-1.5
13. Backing Bar/Inner Hood	88057	2.79	1.48	2.81	1.49	-0.6
14. Backing Bar/Inner Hood	88063	2.79	1.48	2.82	1.49	-0.8
15. Hood Support/Inner Hood	88046	2.83	1.50	2.84	1.50	-0.2
16. Hood Support/Middle Hood	87897	2.78	1.48	2.85	1.51	-2.0
17. Hood Support/Inner Hood	88028	2.84	1.52	2.84	1.52	-0.1
18. Hood Support/Inner Hood	88016	2.94	1.53	2.97	1.55	-1.0
19. Hood Support/Inner Hood	88040	2.96	1.58	2.97	1.59	-0.3
20. Backing Bar/Middle Hood	87826	3.17	1.65	3.18	1.65	0.0
21. Backing Bar/Inner Hood	85455	3.20	1.71	3.20	1.71	0.2
22. Hood Support/Vane Bank/Mid Cover Plate	93159	1.77	1.74	1.77	1.74	0.1
23. Outlet Plenum/Inner Hood	85304	3.24	1.74	3.25	1.74	-0.1
24. Middle Hood Support/Hood	87906	3.21	1.74	3.29	1.78	-2.2
25. Backing Bar/Inner Hood	85256	2.88	1.81	2.89	1.81	-0.1
26. Hood Support/Inner Hood	88049	3.48	1.82	3.48	1.82	-0.2
27. Hood Support/Middle Hood	87806	3.49	1.90	3.56	1.94	-2.1
28. Hood Support/Middle Hood	87909	3.80	1.97	3.82	1.99	-0.8

1. R_{PPD} is the change in stress achieved with PPD.

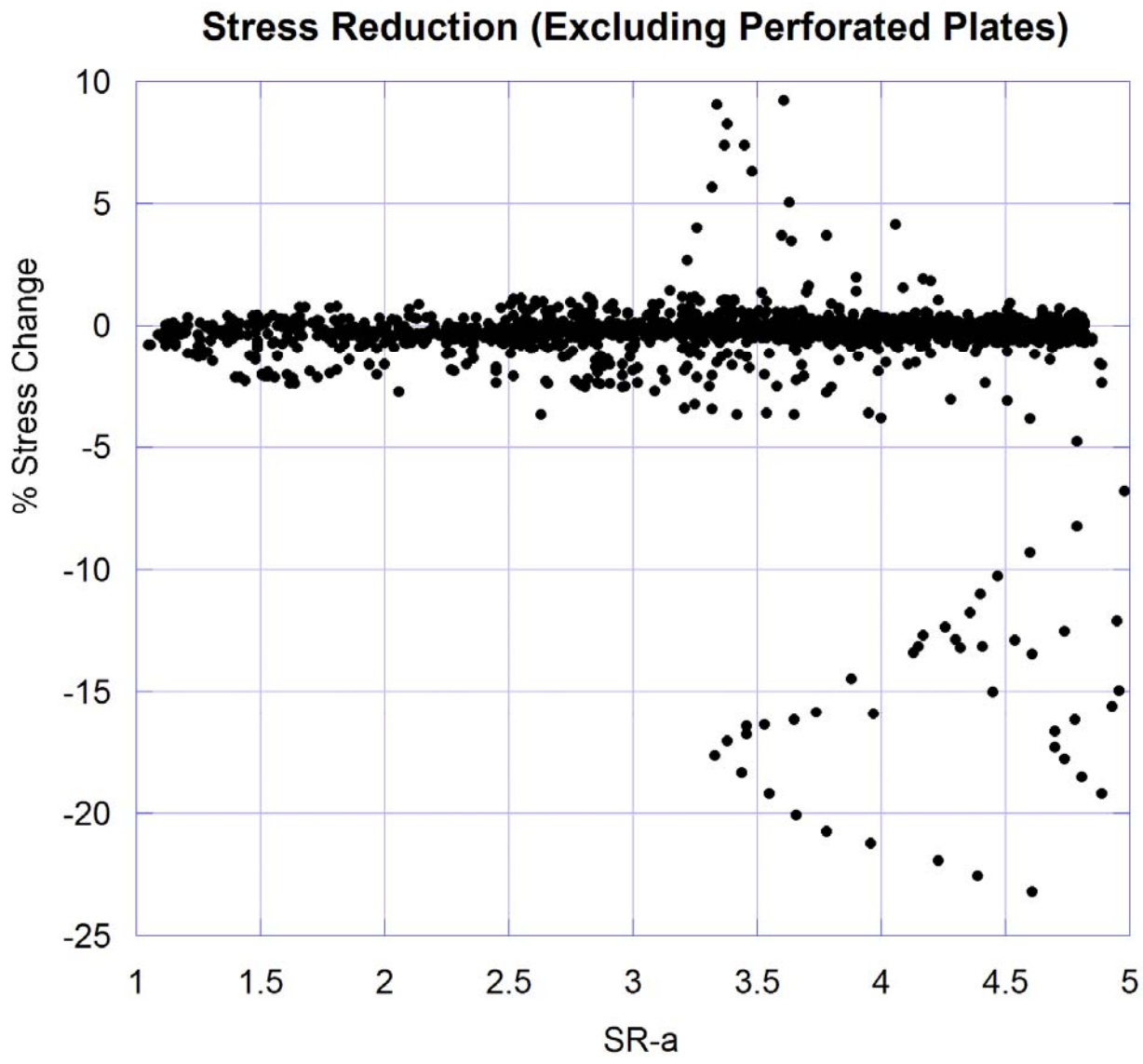

Figure 6. Stress reduction due to PPD at all points with SR-a <5. Perforated plate s themselves are excluded from this list.

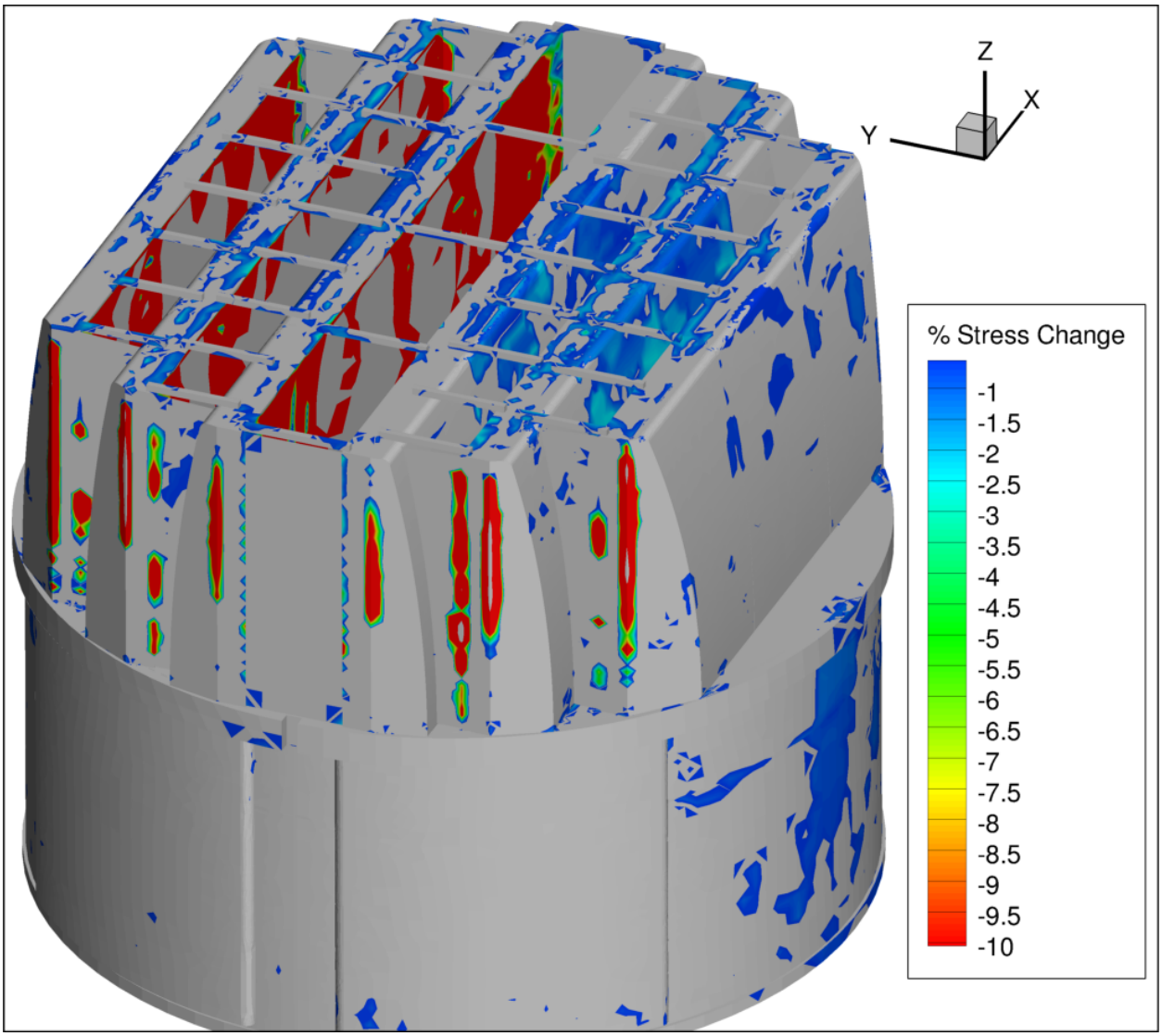

Figure 7a. Distribution of stress reduction on HC1 dryer due to PPD.

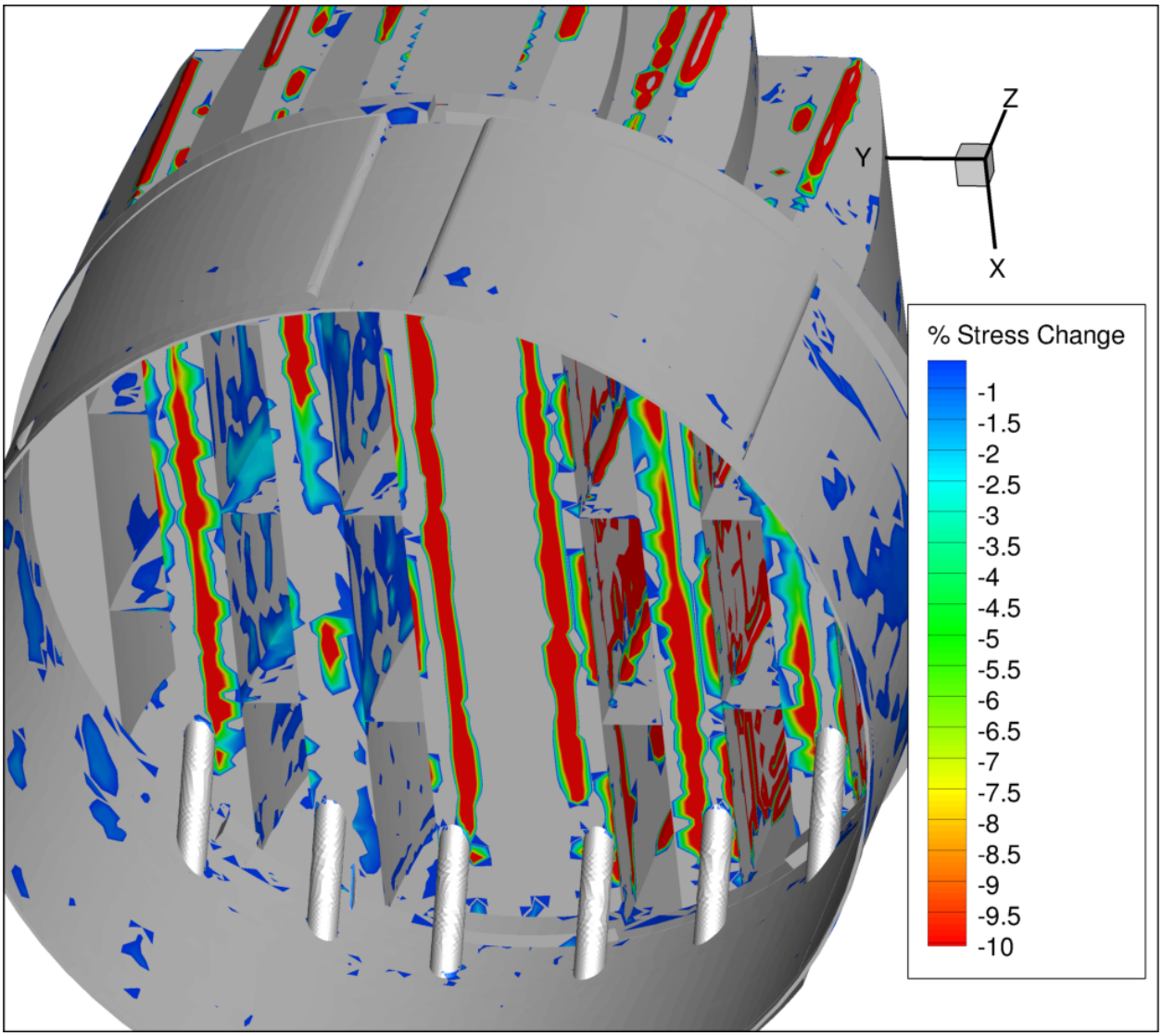

Figure 7b. Distribution of st ress reduction on HC1 dryer due to P PD (second view from underneath the dryer).

4. Conclusions

A harmonic steam dryer stress analysis with perforated plate damping accounted for has been used to calculate high stress locations and stress ratios for the HC1 steam dryer at MUR conditions using plant measurement data. The loads obtained in a separate acoustic circuit model [9], including end-to-end bias and uncertainty [4, 9], were applied to a finite element model of the steam dryer consisting mainly of the ANSYS Shell 63 elements and brick continuum elements. The resulting stress histories were analyzed to obtain alternating and maximum stresses at all nodes for comparison against allowable levels. These results are tabulated in Table 4 of this report and compared against the corresponding predictions without PPD in Table 6. The minimum alternating stress ratio (SR-a) at any frequency shift is 1.05. The most limiting maximum stress intensity stress ratio (SR-P) is 1.25. These results account for all end-to-end biases and uncertainties and meet the ASME code requirements.

On the basis of these MUR plant loads, the dynamic analysis of the steam dryer shows that the combined acoustic, hydrodynamic, and gravity loads produce the following minimum stress ratios:

Frequency Shift	Minimum Stress Ratio	
	Max. Stress, SR-P	Alternating Stress, SR-a
-10%	1.35	1.33
-7.5%	1.34	1.52
-5%	1.35	1.40
-2.5%	1.26	1.11
0% (nominal)	1.33	1.10
+2.5%	1.31	1.05
+5%	1.31	1.22
+7.5%	1.28	1.17
+10%	1.27	1.12
All shifts	1.26 – 1.35	1.05 – 1.52

The limiting stress locations with SR-a<2 are similar to those obtained without PPD. While stress reductions of up to 23% are observed at some significant stress locations (SR-a<5) near the perforated plates and up to 2.6 % for locations with SR-a<1.40, the limiting stress location only sees a stress reduction of 1.2% or an alternating stress ratio increase from SR-a=1.04 without PPD to SR-a=1.05 with PPD. Hence this location on the middle hood/backing bar weld remains the limiting location.

5. References

1. Continuum Dynamics, Inc. (2016) Basis for Modeling Vibration-Induced Loading in Steam Dryers. C.D.I. Technical Note No. 16-16P (Proprietary), Rev. 0, Oct.
2. Continuum Dynamics, Inc. (2016) Stress Evaluation of Hope Creek Unit 1 Steam Dryer at CLTP and MUR Conditions Using 42.5% VIL. C.D.I. Report No. 16-09P (Proprietary), Rev. 0, Oct.
3. Continuum Dynamics, Inc. (2015) Stress Re-Evaluation of Hope Creek Unit 1 Steam Dryer at 115% CLTP. C.D.I. Report No. 15-06P (Proprietary), Rev. 0, Oct.
4. Continuum Dynamics, Inc. (2015) Design Record File DRF-PSEG-352.
5. Continuum Dynamics, Inc. (2007) Finite Element Modeling Bias and Uncertainty Estimates Derived From the Hope Creek Unit 2 Dryer Shaker Test, Revision 0. CDI Report No. 07-27P.
6. Continuum Dynamics, Inc. (2014) Stress Re-Evaluation of Nine Mile Point Unit 2 Steam Dryer at 115% CLTP. C.D.I. Report No. 14-08P (Proprietary), July.
7. Continuum Dynamics, Inc. (2009) Stress Assessment of Browns Ferry Nuclear Unit 1 Steam Dryer to 120% OLTP Power Level, Rev. 0. C.D.I. Report No. 09-25P (Proprietary), August.
8. Continuum Dynamics, Inc. (2007) Dynamics of BWR Steam Dryer Components. C.D.I. Report No. 07-11P.
9. Continuum Dynamics, Inc. (2007) Methodology to Predict Full Scale Steam Dryer Loads from In-Plant Measurements, with the Inclusion of a Low Frequency Hydrodynamic Contribution. C.D.I. Report No. 07-09P (Proprietary).
10. ASME (2007) Boiler and Pressure Vessel Code, Section III, Subsection NG.
11. de Santo, D.F., *Added Mass and Hydrodynamic Damping of Perforated Plates Vibrating In Water.* Journal of Pressure Vessel Technology, 1981. **103**: p. 175-182.
12. Idel'chik, I E. and E. Fried, *Flow Resistance, a Design Guide for Engineers*. 1989, Washington D.C.: Taylor & Francis. pg. 260.

CDI Affidavit supporting the withholding of information in Enclosure 3 from public disclosure

Continuum Dynamics, Inc.

(609) 538-0444 (609) 538-0464 fax 34 Lexington Avenue Ewing, NJ 08618-2302

AFFIDAVIT

RE: CDI Technical Note No. 16-23P "Stress Evaluation of Hope Creek Unit 1 Steam Dryer at MUR Conditions Using Perforated Plate Damping," Revision 0

I, Alan J. Bilanin, being duly sworn, depose and state as follows:

1. I hold the position of President and Senior Associate of Continuum Dynamics, Inc. (hereinafter referred to as CDI), and I am authorized to make the request for withholding from Public Record the Information contained in the document described in Paragraph 2. This Affidavit is submitted to the Nuclear Regulatory Commission (NRC) pursuant to 10 CFR 2.390(a)(4) based on the fact that the attached information consists of trade secret(s) of CDI and that the NRC will receive the Information from CDI under privilege and in confidence.

2. The Information sought to be withheld, as transmitted to PSEG Nuclear LLC as attachment to CDI Letter No. 17077 dated 13 December 2017, CDI Technical Note No. 16-23P "Stress Evaluation of Hope Creek Unit 1 Steam Dryer at MUR Conditions Using Perforated Plate Damping," Revision 0. The proprietary information is identified by its enclosure within pairs of double square brackets ("[[ ]]"). In each case, the superscript notation $^{(3)}$ refers to Paragraph 3 of this affidavit that provides the basis for the proprietary determination.

3. The Information summarizes:

   (a) a process or method, including supporting data and analysis, where prevention of its use by CDI's competitors without license from CDI constitutes a competitive advantage over other companies;
   (b) Information which, if used by a competitor, would reduce his expenditure of resources or improve his competitive position in the design, manufacture, shipment, installation, assurance of quality, or licensing of a similar product;
   (c) Information which discloses patentable subject matter for which it may be desirable to obtain patent protection.

   The information sought to be withheld is considered to be proprietary for the reasons set forth in paragraphs 3(a), 3(b) and 3(c) above.

4. The Information has been held in confidence by CDI, its owner. The Information has consistently been held in confidence by CDI and no public disclosure has been made and it is not available to the public. All disclosures to third parties, which have been limited, have been made pursuant to the terms and conditions contained in CDI's Nondisclosure Secrecy Agreement which must be fully executed prior to disclosure.

5. The Information is a type customarily held in confidence by CDI and there is a rational basis therefore. The Information is a type, which CDI considers trade secret and is held in confidence by CDI because it constitutes a source of competitive advantage in the competi ion and performance of such work in the industry. Public disclosure of the Information is likely to cause substantial harm to CDI's competitive position and foreclose or reduce the availability of profit-making opportunities.

I declare under penalty of perjury that the foregoing affidavit and the matters stated therein are true and correct to be the best of my knowledge, information and belief.

Executed on this 13th day of December 2017.

Alan J. Bilanin
Continuum Dynamics, Inc.

Subscribed and sworn before me this day: 13 December 2017

Eileen P. Burmeister, Notary Public

EILEEN P BURMEISTER
ID # 2201169
NOTARY PUBLIC
STATE OF NEW JERSEY
My Commission Expires May 6, 2022